iScience

CellPress
OPEN ACCESS

Article

Prx4 acts as DAMP in shrimp, enhancing bacterial resistance via the toll pathway and prophenoloxidase activation

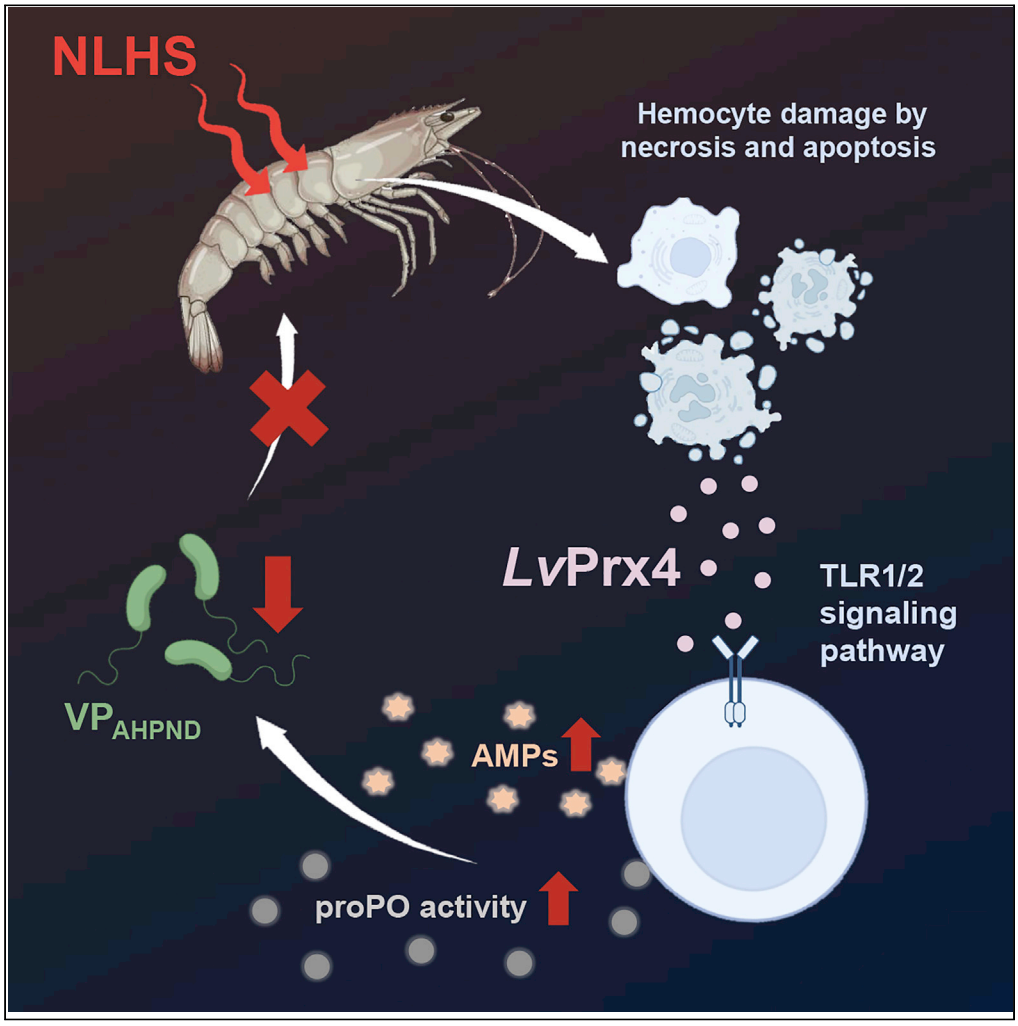

Supitcha Wanvimonsuk, Phattarunda Jaree, Taro Kawai, Kunlaya Somboonwiwat

kunlaya.s@chula.ac.th

Highlights

Heat stress induces shrimp hemocyte necrosis and early apoptosis

*Lv*Prx4 was upregulated in hemocyte and released into hemolymph on heat stress

*Lv*Prx4 acts as DAMP, enhancing resistance to VP_{AHPND} infection in shrimp

*Lv*Prx4 activates the TLR1/2 signaling pathway and the proPO activating system

Wanvimonsuk et al., iScience *26*, 105793
January 20, 2023
https://doi.org/10.1016/j.isci.2022.105793

iScience

CellPress
OPEN ACCESS

Article

Prx4 acts as DAMP in shrimp, enhancing bacterial resistance via the toll pathway and prophenoloxidase activation

Supitcha Wanvimonsuk,[1] Phattarunda Jaree,[2] Taro Kawai,[3] and Kunlaya Somboonwiwat[1,4,*]

SUMMARY

Peroxiredoxin (Prx), an antioxidant enzyme family, has been identified as immune modulating damage-associated molecular patterns (DAMPs) in mammals but not in shrimp. Acute non-lethal heat shock (NLHS) that enhances shrimp *Penaeus vannamei* resistance to *Vibrio parahaemolyticus* causing acute hepatopancreatic necrosis disease (VP_{AHPND}). Among the five *P. vannamei* Prxs (*Lv*Prx) isoforms, *Lv*Prx4, the most abundant in unchallenged shrimp hemocytes that was upregulated in hemocytes following NLHS treatment, is of great interest. The escalation of the *Lv*Prx4 monomer in hemolymph of NLHS treated shrimp indicates that it probably acts as DAMP. This study revealed that pre-challenge with r*Lv*Prx4 could prolong VP_{AHPND}-infected shrimp survival, increase prophenoloxidase (proPO) activity and promote Toll pathway-related genes expression mediated by Toll-like receptor (TLR) 1 and 2. The presented findings elucidated the molecular mechanism of *Lv*Prx4 monomer as DAMP in NLHS-induced VP_{AHPND} resistance by inducing the TLR1/2 signaling pathway and the proPO activating system.

INTRODUCTION

Shrimp defend themselves against pathogen invasion by triggering cellular and humoral responses of innate immunity, in which hemocytes contribute significantly. Cellular immune responses include nodulation, encapsulation, apoptosis, and phagocytosis, whereas humoral immune responses consist of the prophenoloxidase (proPO) activating system and production of antimicrobial peptides (AMPs). The immune response is initiated when triggered by pathogen-associated molecular patterns (PAMPs) such as lipopolysaccharide, β-1,3-glucan, and peptidoglycan. PAMPs are recognized by pattern recognition protein (PRP) or receptor (PRR). The signal is transmitted through intracellular signaling proteins of different immune-related pathways, e.g., Toll pathway, Imd pathway, and JAK/STAT pathway.[1]

Stress-induced cell damage causes the release of endogenous molecules known as damage-associated molecular patterns (DAMPs), which can promote infection-independent immune responses.[2] The best-known DAMPs are high-mobility group box (HMGB) proteins, interleukins such as IL-1α, cytosolic calcium-binding proteins of the S100 family, heat-shock proteins (HSPs), and nucleosomes[3] as well as intracellular components released from cell death or necrosis cell such as ATP, uric acid, RNA, and DNA.[4] Despite mounting evidence that DAMPs play a role in modulating innate immunity, the mechanistic basis of this function in shrimp remains unknown.

The major cultured shrimp species, *Penaeus vannamei*, accounts for the majority of world aquaculture market share. Infectious diseases, particularly acute hepatopancreatic necrosis (AHPND) caused by *Vibrio parahaemolyticus* (VP_{AHPND}), pose significant risks to the aquaculture industry. Because of the availability of the genome sequence[5] and the efficacy of antibacterial immunity exhibited in shrimp, we believe *P. vannamei* is a promising model system for exploring the molecular basis of DAMP activating infection-independent immune responses.[1,6,7]

Exposure to temperature above normal ambient condition or non-lethal heat shock (NLHS) can enhance resistance and/or tolerance to pathogen infections in many organisms. The NLHS applied to brine shrimp *Artemia franciscana*, induces protection of the Artemia larvae against *Vibrio campbellii* and *Vibrio proteolyticus* with survival enhanced 2-fold over non-heated animals and NLHS-treated brine shrimp.[6,7]

[1]Center of Excellence for Molecular Biology and Genomics of Shrimp, Department of Biochemistry, Faculty of Science, Chulalongkorn University, Bangkok 10330, Thailand

[2]Center of Applied Shrimp Research and Innovation, Institute of Molecular Biosciences, Mahidol University, Salaya, Nakhon Pathom 73170, Thailand

[3]Laboratory of Molecular Immunobiology, Nara Institute of Science and Technology, Nara 630-0192, Japan

[4]Lead contract

*Correspondence: kunlaya.s@chula.ac.th

https://doi.org/10.1016/j.isci.2022.105793

Short-term hyperthermic treatment of the black tiger shrimp, *Penaeus monodon*, can reduce replication of gill associated virus.[8] Asian green mussel *Perna viridis* becomes more thermotolerance and resistance to *Vibrio alginolyticus* after NLHS treatment.[9] Moreover, the acute and chronic NLHS enhances *P. vannamei*, tolerance to VP_{AHPND} infection by the induction of *Lv*HSP70, *Lv*HSP90 and subsequent activation of the proPO system.[10] Transcriptomic data of NLHS-induced *P. vannamei* revealed that miRNA and mRNA interactions contribute to the modulation of NLHS-induced immune responses, such as the prophenoloxidase-activating system, hemocyte homeostasis, and antimicrobial peptide production.[11] However, the role of an antioxidant enzyme in NLHS-induced immune responses remains elusive.

The peroxiredoxin (Prx) family, also recognized as DAMPs in mammals, is an antioxidant enzyme that controls cytokine-induced peroxide levels and thus mediates signal transduction. Prxs are classified into three subtypes based on the type of catalytic cysteine: 2-Cys typical, 2-Cys atypical and 1-Cys. Six family members, Prx1-6, have been reported in humans. Circulating Prx1 is a DAMP for acute liver injury that induces the expression of pro-IL-1, IL-6, TNF, and IL-1 via NF-κβ and inflammasome signaling pathway.[12] Several DAMPs have been shown to activate inflammatory cells via Toll-like receptor (TLR) 2 and TLR4. Prx is one of the strong DAMPs that activates infiltrating macrophages in brain ischemia via TLR2 and TLR4.[13] Prx2 is also classified as a danger signal because it acts as a redox-dependent immune mediator, triggering macrophage to cause TNF-α production and release.[14,15] The *Prx* from Antarctic Sea urchin, *Sterechinus neumayeri*, which is involved in the antioxidant response, was found to be up-regulated after a *Vibrio anguillarum* challenge and heat stress.[16] In addition, *Prx5* from ridgetail white prawn, *Exopalaemon carinicauda*, is involved in immune response against bacterial and viral infection, as implied by the up-regulation of gene expression both in hemocytes and hepatopancreas after *V. anguillarum* and WSSV challenge.[17]

In this study, we identified *Prx* genes (*LvPrx*) from the *P. vannamei* genome database and investigated the molecular mechanism of a major *LvPrx* isoform expressed in hemocyte, *LvPrx4*, in enhancing immunity against VP_{AHPND} of NLHS-induced *P. vannamei*. As a result of *Lv*Prx4 protein release into the hemolymph in response to NLHS, we explored whether it acts as a DAMP, signaling TLR receptors and modulating other immune-related pathways. These findings pave the way for the development of an immunostimulant-based strategy to enhance culture shrimp resistance to pathogenic microorganisms.

RESULTS

Acute-NLHS stress increases cell death in shrimp hemocytes

Non-lethal heat shock (NLHS) has been preciously demonstrated inducing various immune pathways in shrimp hemocytes.[11] The effect of NLHS was thus initially examined on shrimp hemocyte cell death. Shrimp hemocytes were subjected to heat stress *in vitro* and the apoptotic and necrosis cell death rate was then determined. It was observed that when exposed to heat, hemocyte necrosis increased while apoptosis decreased (Figure 1A). Similarly, an *in vivo* study demonstrated that shrimp hemocytes subjected to acute-NLHS treatment and subsequently restored to ambient temperature presented a 2.8-fold higher number of necrosis cells but a 0.9-fold lower number of apoptotic cells 3 h after recovery (Figure 1B). It should be noted that in apoptotic cell death, the number of early apoptotic cells increased whereas those of late apoptotic cells decreased. In addition, the *caspase3* gene, a key mediator of apoptosis, was down-regulated in response to acute-NLHS, whereas the *inhibitor of apoptosis* gene was upregulated (Figure 1C), corresponding to the lower level of apoptotic cells observed. Based on previous studies, necrosis and early apoptosis allow the release of DAMP protein.[18] Necrosis and early apoptosis in hemocytes triggered by acute-NLHS might thus lead to the release of danger signals that will result in the activation of immune responses.

P. vannamei peroxiredoxin (Prx) is a five-member family

Prx is among the strong danger signals in humans[12,19–21] but no information is available for shrimp. This study aimed at discovering whether *Lv*Prx is an NLHS-induced molecule that can activate an innate immune response against VP_{AHPND} infection. After examining the genome database of *P. vannamei*,[5] five *Lv*Prx isoforms including *Lv*Prx1, *Lv*Prx3, *Lv*Prx4, *Lv*Prx5, and *Lv*Prx6, were identified. The phylogenetic analysis of *Lv*Prx protein demonstrated that *Lv*Prx1, *Lv*Prx3 and *Lv*Prx4 were clustered into the same clade whereas *Lv*Prx5 and *Lv*Prx6 were grouped separately (Figure S1). These isoforms can be thus divided into three subtypes based on the conserved cysteine residues directly associated with the catalytic mechanism and the conserved regions around catalytic residues: 2-Cys typical (*Lv*Prx1, *Lv*Prx3 and *Lv*Prx4), atypical (*Lv*Prx5) and 1-Cys (*Lv*Prx6). Amino acid sequence alignment revealed that all *Lv*Prxs contain the conserved residues

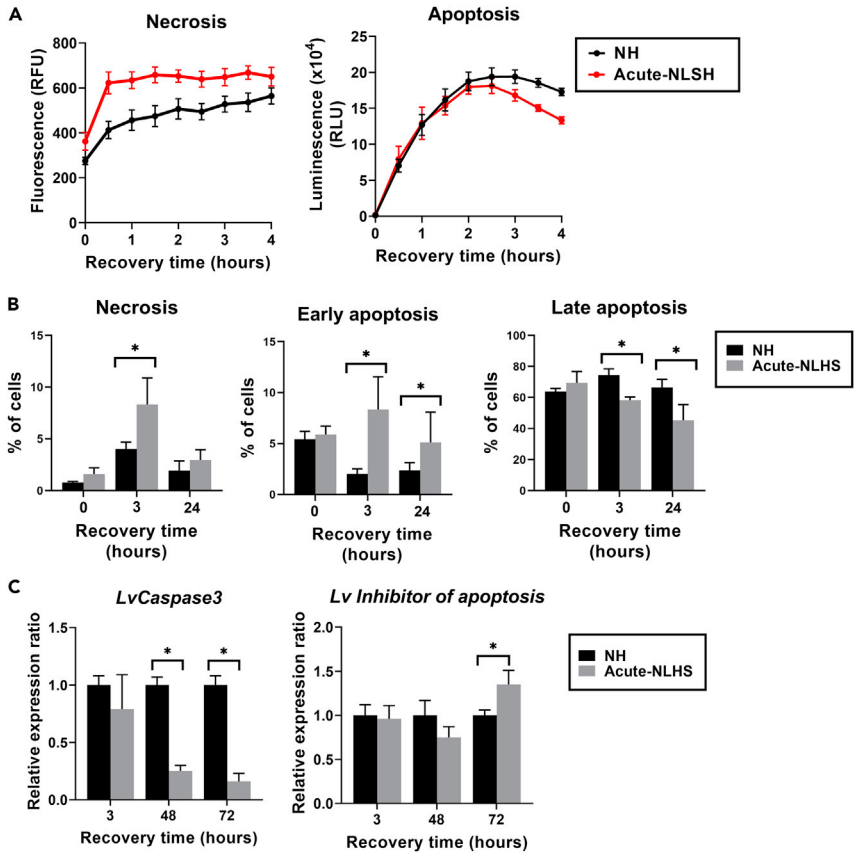

Figure 1. Acute-NLHS treatment induced hemocyte cell death

(A and B) Necrosis and apoptosis of acute-NLHS treated (Acute-NLHS) or non-heated (NH) shrimp hemocyte at 0–4 h recovery was analyzed using (A) Realtime-Glo annexin V apoptosis and necrosis assay and (B) flow cytometry. Experiments were performed in triplicates and presented as means ± SD values at each time point.

(C) The expression levels of *LvCaspase3* and *Lv Inhibitor of apoptosis* genes in hemocyte of acute-NLHS group were quantified using qRT-PCR in comparison with the non-heated (NH) group. The *EF-1α* was utilized as an internal control. The bar graphs correspond to mean ± SD values and asterisk indicates statistically significant difference ($p < 0.05$).

required for the enzymatic activity, including peroxidatic cysteine (Cp), proline (P) and threonine (T) (Figure S2). It should be noted that only *Lv*Prx1 and *Lv*Prx4 containing resolving cysteine (Cr). *Lv*Prx4 is the only member with a signal peptide at the N-terminus, suggesting that it might be a secretory protein (Figure 2A).

LvPrx4 is the most abundant isoform in hemocytes upregulated by acute-NLHS

Distribution of *LvPrxs* in different tissues (heart, hepatopancreas, gills, muscle, intestines, stomach and lymphoid) was examined in healthy shrimp by semi-quantitative RT-PCR (Figure S3). The results showed that all *LvPrx* isoforms were expressed differently in the examined tissues. *LvPrx4* is the most abundant isoform in hemocytes, which is one of the key immune tissues in shrimp. *LvPrxs* expression pattern analysis in *P. vannamei* following recovery from acute-NLHS treatment demonstrated that *LvPrx3* and *LvPrx4* were significantly upregulated following NLHS treatment whereas *LvPrx3* demonstrated the highest fold change (8.9-fold at 48 h and 2.6 h after recovery) although it presented lowest copy number detected (Figure 2B). This study thus focused on *LvPrx4*, the most abundant isoform with significant upregulation of hemocytes transcript levels in hemocytes, to assess its participation in shrimp resistance to AHPND following acute-NLHS treatment.

The effect of acute-NLHS treatment on the localization of *Lv*Prx4 protein in hemocytes and hemolymph was then determined. Immunofluorescence of hemocytes following a 72-h recovery from acute-NLHS treatment suggested that *Lv*Prx4 was distributed selectively in the cytoplasm of hemocytes from both

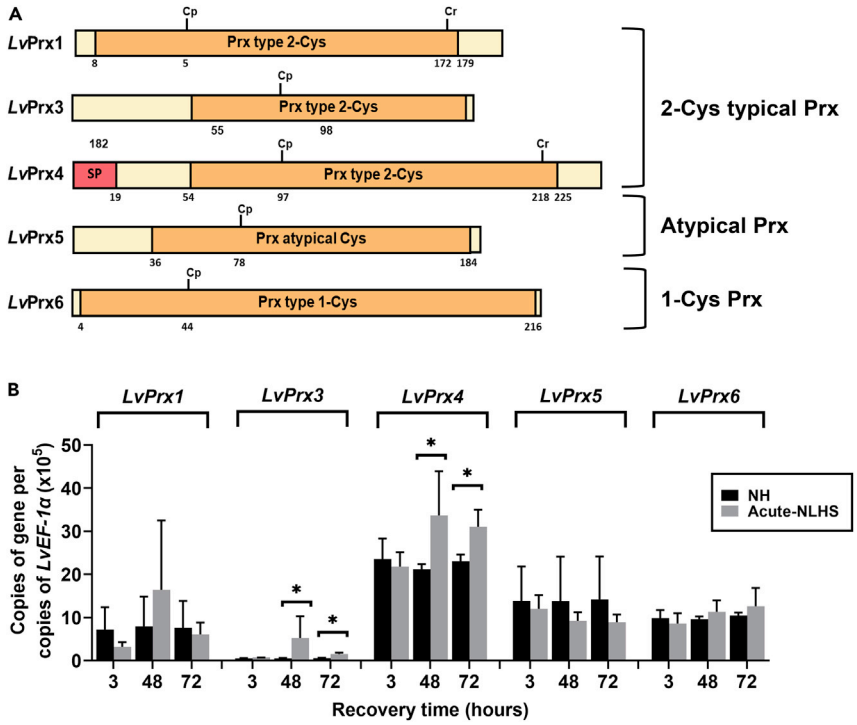

Figure 2. Five isoforms of *LvPrxs* and the expression patterns of *LvPrxs*after acute-NLHS

(A) Analysis of the conserved domains (CD) in the *Lv*Prxs amino acid sequence discovered by CD-search in NCBI. The conserved domains of Prxtype 2-Cys, Prxtype 1-Cys, and Prx atypical Cys, were found. SP indicates signal peptide.

(B) Expression was quantified by qRT-PCR compared to the non-heated (NH) group. The *EF-1α* was utilized as an internal control. Values are expressed as means ± SDs and the asterisk indicates statistically significant difference ($p < 0.05$).

non-heated and acute-NLHS treated shrimp. Furthermore, *Lv*Prx4 expression was not limited in a specific type of hemocyte (Figure 3A). The *Lv*Prx4 dimer increased over the recovery time (from 3 to 72 h) after acute-NLHS in hemocytes (Figure 3B). Moreover, the released *Lv*Prx4 monomer was detected in acute-NLHS treated hemolymph (Figure 3C) that corresponded to higher peroxidase activity observed in hemolymph (Figure 3D). These findings indicate that *Lv*Prx4 produced in hemocytes and released into hemolymph as a monomer following acute-NLHS treatment is functionally active.

*Lv*Prx4 is an antioxidant enzyme that protects cell from oxidative damage

Recombinant *Lv*Prx4 protein (r*Lv*Prx4) was produced, purified, and used in functional assays (Figure S4A). Based on the pyrogallol assay, purified r*Lv*Prx4 presents peroxidase activity of approximately 36 units/μl (Figure S4B). The ROS removal activity of r*Lv*Prx4 was determined by a metal-catalyzed oxidation (MCO) assay. The ROS radicals produced in the MCO assay using DTT and $FeCl_3$ can trigger nicks in supercoiled plasmids that can be detected as a shift in the plasmid gel mobility. Following a 2-h incubation, purified r*Lv*Prx4 could prevent supercoiled DNA nicking in a dose-dependent manner (Figure S4C). When r*Lv*Prx4 was replaced with the control protein, rGST, the reaction could not lead to ROS removal and resulted in damage of the plasmid. This finding suggests that *Lv*Prx4 has a role as an antioxidant enzyme protecting oxidative DNA damage from oxidants.

*Lv*Prx4 participates in AHPND resistance enhancement

To better understand the role of *Lv*Prx4 in VP_{AHPND} resistance in shrimp, *LvPrx4* silencing was performed using the RNAi technique. The dsRNAs specific to *LvPrx4* (dsPrx4), GFP (dsGFP) as a control of dsRNA, 0.85% NaCl as an injection control, were injected into shrimp. After a period of 24 h post-injection, the relative expression of *LvPrx4* gene in hemocytes was determined using qRT-PCR where approximately 70% suppression was observed (Figure S5). The percent survival of the *LvPrx4* knockdown and the control shrimp challenged with 5×10^5 CFU/mL VP_{AHPND} was then assessed (Figure 4A). Suppression of *LvPrx4* expression resulted in lower survival rate compared to infection controls injected with dsGFP and NaCl.

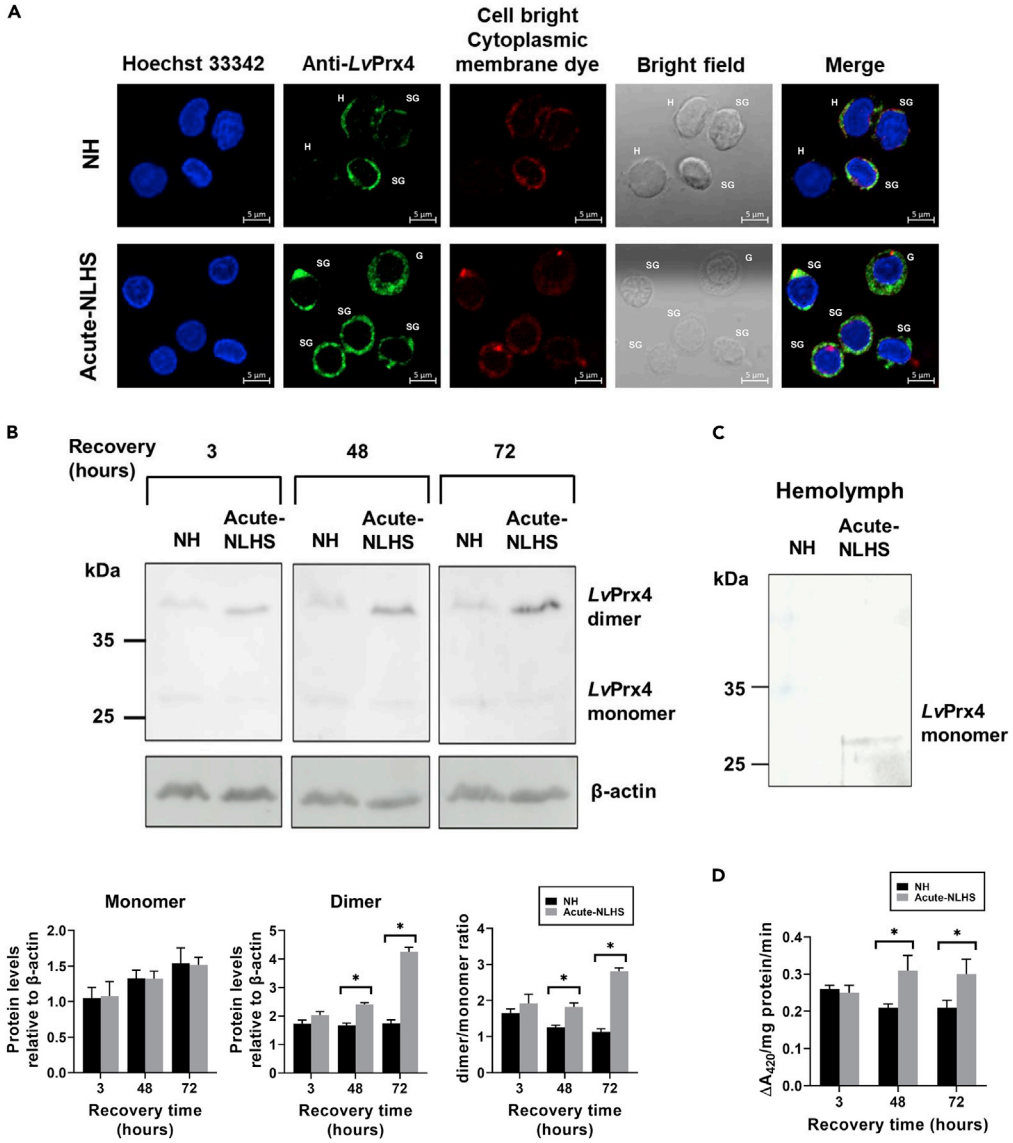

Figure 3. *Lv*Prx4 was upregulated following acute-NLHS treatment

(A–C) Localization of *Lv*Prx4 on shrimp hemocytes; hyalin (H), semi-granular, and granular (G) cells, by immunofluorescence. The nucleus, cytoplasmic membrane and *Lv*Prx4 are stained in blue (Hoechst 33,342), red (CellBrite cytoplasmic membrane) and green (Alexa Fluor 488) colors, respectively. Western blot analysis of *Lv*Prx4 in NLHS treated (B) hemocyte at 3 h, 48 h, and 72 h recovery (C) hemolymph following a 72-h recovery.

(D) Peroxidase activity in shrimp hemolymph following NLHS treatment by pyrogallol assay. Bar graphs demonstrate mean ± SD values and the asterisk suggests statistically significant difference ($p < 0.05$).

It should be noted those non-infected controls survived throughout the experiment. The results presented above suggest that *Lv*Prx4 did not only function as an antioxidant enzyme but also played a significant role during VP_{AHPND} infection.

To study the impact of the r*Lv*Prx4 protein on shrimp resistance to VP_{AHPND} infection, shrimp were injected with 2 nmol/g shrimp r*Lv*Prx4, 2 nmol/g shrimp rGST or 20 mM Tris pH 8.0 buffer. After a period of 24 h post-r*Lv*Prx4 injection, shrimp were challenged with 5×10^5 CFU/mL VP_{AHPND} by immersion. Pre-injection with r*Lv*Prx4 extended survival of VP_{AHPND} challenged shrimp compared with the control groups. Shrimp survival in VP_{AHPND} infection control groups dropped to 0% within 78 h whereas the pre-r*Lv*Prx4 challenged shrimp survived longer (102 h after infection) (Figure 4B). In addition, hemolymph and hepatopancreas of

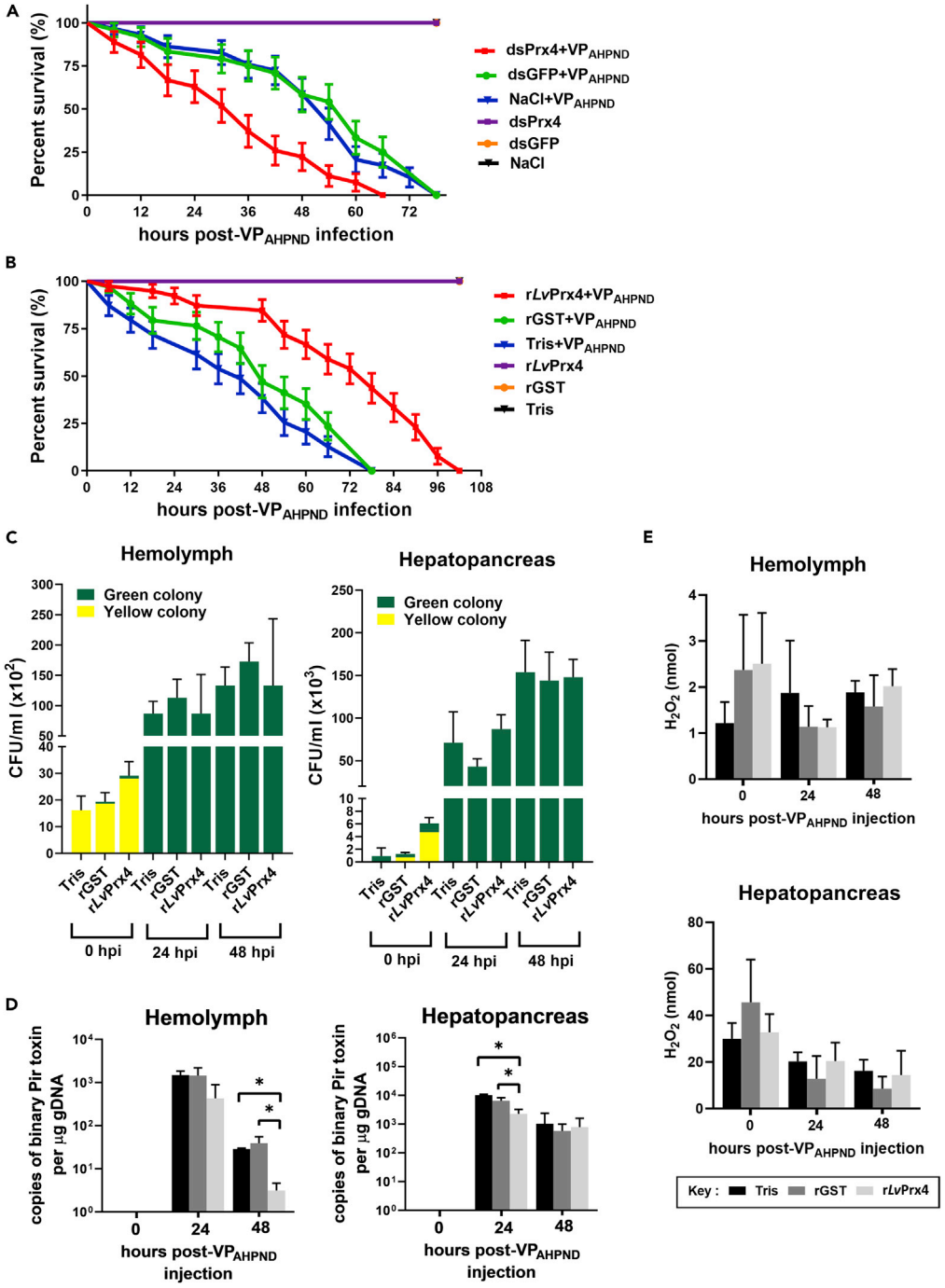

Figure 4. Protective effect of r*Lv*Prx4 on VP$_{AHPND}$challenge in shrimp

(A) *LvPrx4* knockdown shrimp were challenged with VP$_{AHPND}$ 5 × 10^5 CFU/mL by immersion.

(B) Shrimp were injected with r*Lv*Prx4, rGST or Tris-Cl buffer. Following a 24 h period post-injection, shrimp were challenged with 5 × 10^5 CFU/mL of VP$_{AHPND}$ by immersion.

(C) Bacteria counting in hemocyte and hepatopancreas by dotting on TCBS agar.

(D) Binary Pir toxin sequence copy number in hemocyte and hepatopancreas.

(E) Determination of H_2O_2 levels by $TiCl_4$ assay at various time points following VP$_{AHPND}$ infection. The bar graphs demonstrate mean ± SD values and asterisk suggests statistically significantly difference ($p < 0.05$).

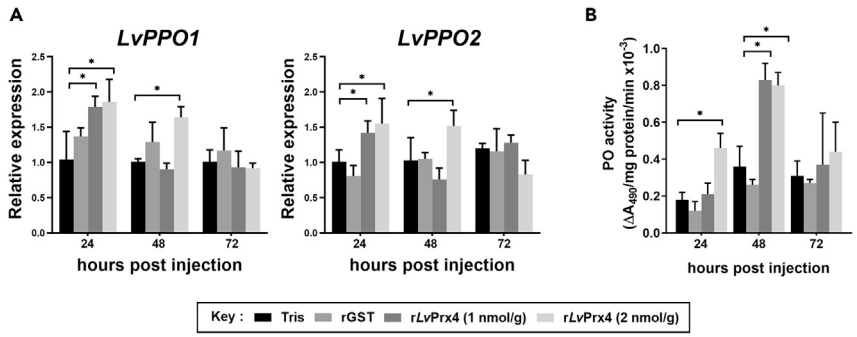

Figure 5. r*Lv*Prx4 could increase prophenoloxidase (PO) activity

(A) The genes of the prophenoloxidase-activating system in the r*Lv*Prx-injected shrimp at various time points following infection were quantified by qRT-PCR compared with the corresponding controls (rGST and 20 mM Tris-Cl pH 8.0). The *EF-1α* was utilized as an internal control.

(B) PO activity in hemolymph protein of the r*Lv*Prx-injected shrimp at various time points following infection. Bar graphs demonstrate mean ± SD values and the asterisk suggests statistically significant difference ($p < 0.05$).

VP_{AHPND} challenged shrimp at 0, 24 and 48 h post infection, were collected to evaluate the number of bacteria using the plate count technique. No difference in bacteria number was observed between the r*Lv*Prx4-injected group and the control group (Figure 4C). Moreover, VP_{AHPND} copy number was also determined whereas the lower amount of VP_{AHPND} in r*Lv*Prx4-injected shrimp was observed as expected (Figure 4D). Importantly, a significantly lower copy number of binary Pir toxin in hemolymph (at 48 h post-VP_{AHPND} challenge) and hepatopancreas (at 24 h post-VP_{AHPND} challenge) of r*Lv*Prx4-injected group was observed, suggesting that a bacterial clearance effect occurred in hemolymph and hepatopancreas. In contrast, r*Lv*Prx4 injection did not affect H_2O_2 content in hemolymph and hepatopancreas (Figure 4E). The above results provide evidence of a *Lv*Prx4 enhancement in AHPND resistance that was not caused primarily by r*Lv*Prx4 antioxidant activity. The r*Lv*Prx-induced immune genes and pathways correlated with AHNPD resistance mechanism in shrimp was then further detected.

A r*Lv*Prx4 injection induces phenoloxidase (PO) activity in shrimp

As prophenoloxidase (proPO) system is one of the key humoral immune responses that fight foreign microbes in invertebrates. Furthermore, ProPO is implicated in the melanin synthesis and production of various reactive intermediates with antimicrobial activities.[1,22] In the present study, it was determined whether r*Lv*Prx4 injection could induce phenoloxidase (PO) activity in shrimp. Following r*Lv*Prx4 injection, *LvPPO1* and *LvPPO2* expression levels were upregulated (Figure 5A) corresponding to a significant increase of PO activity after a 24 to 48 h period post-r*Lv*Prx4 injection compared to the corresponding controls (Figure 5B). *Lv*Prx4 could thus enhance the proPO system that is associated with an increased resistance to VP_{AHPND} infection in shrimp.

*Lv*Prx4 acts as a signal to activate immune signaling pathway

Of interest, expression profiling of key immune-related genes in hemocytes revealed that a r*Lv*Prx4 injection could stimulate the expression of other immune-related genes (Figure 6). A challenge with either 1 or 2 nmol r*Lv*Prx4/g shrimp resulted in a significant increase in expression of key genes of the Toll pathway (*LvMyD88*, *LvPelle*, *LvTRAF6* and *LvDrosal*) 24 h post-injection and a decrease later. The Imd pathway components (*LvIMD*, *LvIKKε*, *LvIKKß* and *LvRelish*) and the JAK/STAT pathway components (*LvDome* and *LvStat*) in contrast, were not upregulated following a r*Lv*Prx4 injection (Figure S6). Of interest, the expression of two antimicrobial peptides (AMPs), penaeidin4 (*LvPEN4*) and anti-lipopolysaccharide factor AA-K (*LvALF AA-K*), were also significantly upregulated following a r*Lv*Prx4 injection. When considering the interferon regulatory factor (IRF)-Vago pathway,[23] the mRNA expression of *Lv*IRF, a transcription factor, was slightly upregulated following a r*Lv*Prx4 injection, 24 h post-injection. Previous studies have demonstrated that an interferon (IFN)-like protein, *Lv*Vago5 is transcriptionally regulated by *Lv*IRF and it plays a key role in shrimp response following VP_{AHPND} infection.[24,25] Consistent with *Lv*IRF expression, a remarkable upregulation of *LvVago5* at the same time point following r*Lv*Prx4 injection was observed. These results indicate that *Lv*Prx4 could trigger the Toll pathway-mediated AMP production as well as the IRF-Vago pathway.

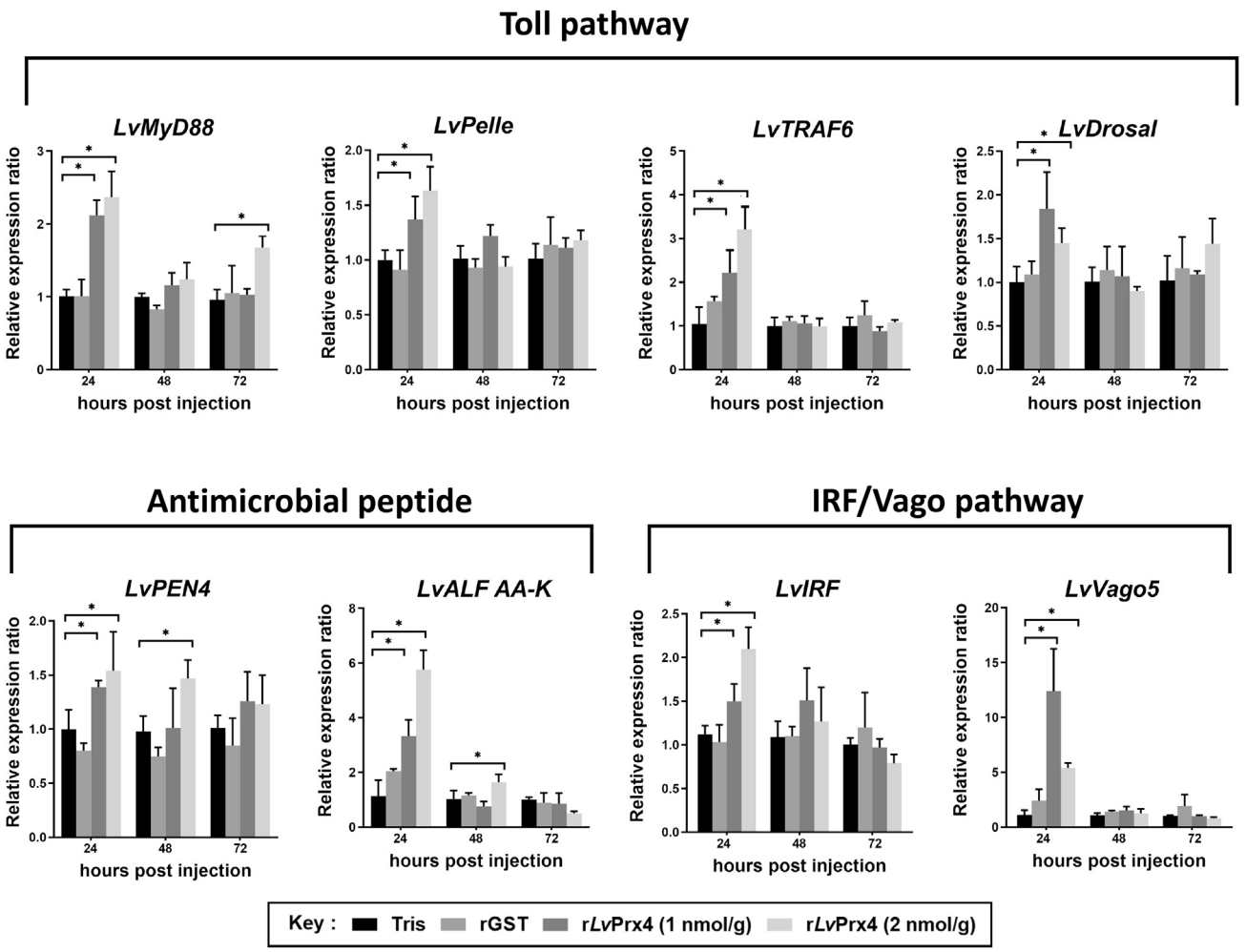

Figure 6. r*Lv*Prx4 injection into shrimp could induce the expression of immune-related genes

Toll pathway, IRF/Vago pathway, and antimicrobial peptide genes were analyzed for their relative expression following a r*Lv*Prx4 injection using qRT-PCR. *EF-1α* was utilized as an internal control. Bar graphs demonstrate mean ± SD values and the asterisk suggests statistically significant difference ($p < 0.05$).

*Lv*Prx4 promotes the expression of immune-related genes mediated by toll-like receptor (TLR)

The contribution of Toll-like receptors (TLR) in regulating the mRNA expression of AMPs and IFN-like protein was then further verified. The expression of *LvTLR1* and *LvTLR2* were observed to be increased in r*Lv*Prx4-injected shrimp (Figure 7A). Localization of either EGFP-tagged leucine rich repeat domain (LRR) of *Lv*TLR1 (*Lv*TLR1_LRR_EGPF) or *Lv*TLR2 (*Lv*TLR2_LRR_EGFP) with *Lv*Prx4 were determined in HEK293T cells using immunofluorescence Figure 7B). *Lv*Prx4 (red fluorescence) co-localized with both *Lv*TLR1_LRR_EGPF and *Lv*TLR2_LRR_EGFP (green fluorescence) in cytoplasm was detected as yellow fluorescence signal in which co-localization of *Lv*Prx4 with *Lv*TLR2_LRR_EGFP demonstrates significantly higher intensity. The results suggest that *Lv*Prx4 activate the Toll pathway through direct interactions with the LRR domain of *Lv*TLR1 and *Lv*TLR2.

LvTLR1 and *LvTLR2* were silenced using specific dsRNA in shrimp hemocyte (Figure S7) and the localization on hemocyte of r*Lv*Prx4-injected into shrimp was then analyzed. Fluorescent images demonstrated that r*Lv*Prx4 injected into shrimp (green fluorescence) was localized on the hemocyte cell surface in dsGFP-treated shrimp. Nevertheless, r*Lv*Prx4 could hardly be detected in dsTLR1-and dsTLR2-treated shrimp (Figure 7C). Based on the above, it could be suggested that *Lv*TLR1 and *Lv*TLR2 in hemocytes are the receptors of *Lv*Prx4.

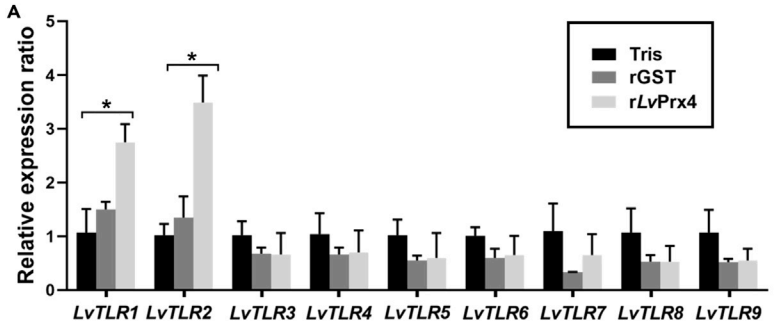
A
Relative expression ratio
Tris
rGST
rLvPrx4
*
*
LvTLR1
LvTLR2
LvTLR3
LvTLR4
LvTLR5
LvTLR6
LvTLR7
LvTLR8
LvTLR9

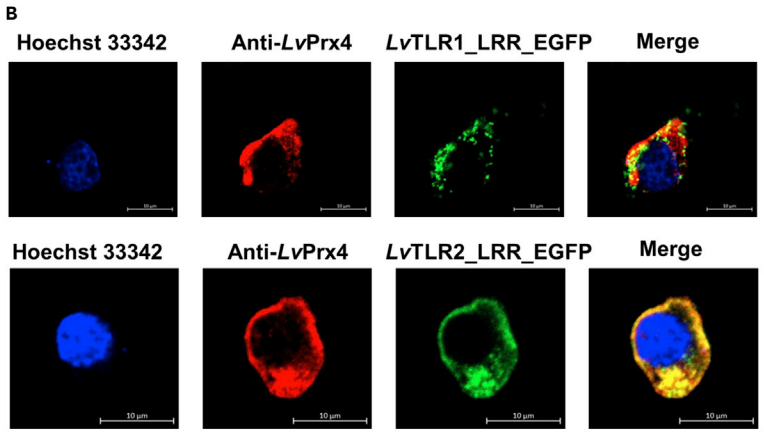
B
Hoechst 33342
Anti-LvPrx4
LvTLR1_LRR_EGFP
Merge
Hoechst 33342
Anti-LvPrx4
LvTLR2_LRR_EGFP
Merge

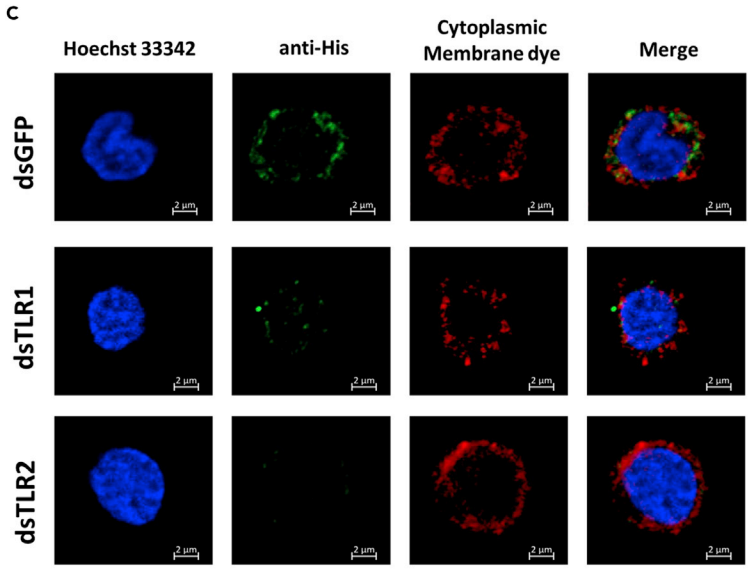
C
Hoechst 33342
anti-His
Cytoplasmic Membrane dye
Merge
dsGFP
dsTLR1
dsTLR2

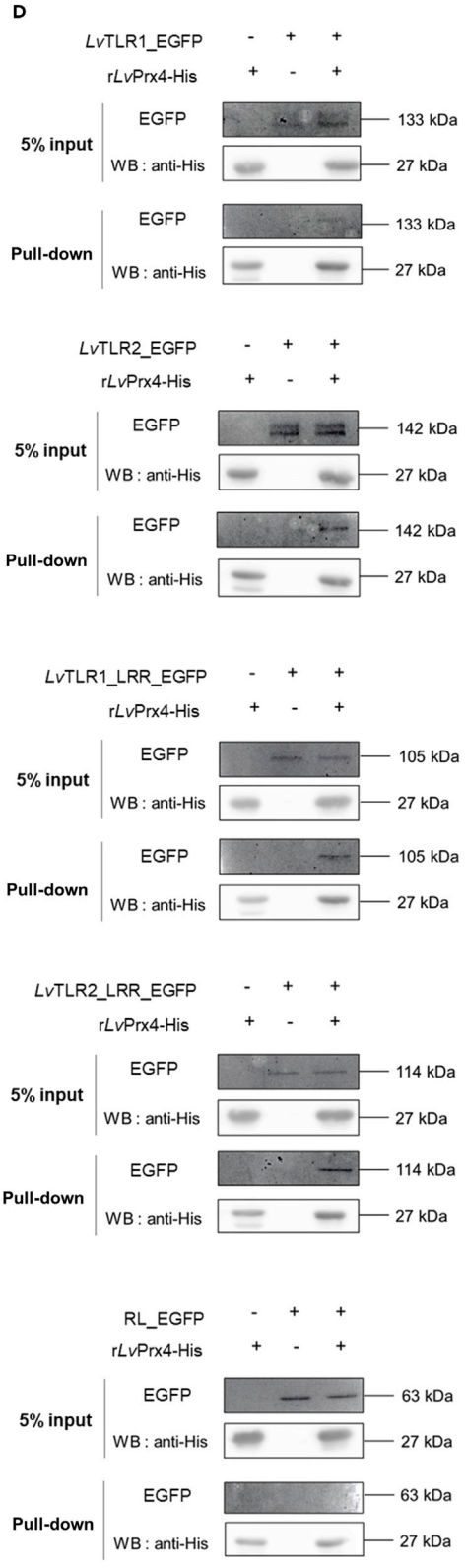
D
LvTLR1_EGFP
rLvPrx4-His
5% input
Pull-down
EGFP
WB : anti-His
133 kDa
27 kDa
LvTLR2_EGFP
142 kDa
LvTLR1_LRR_EGFP
105 kDa
LvTLR2_LRR_EGFP
114 kDa
RL_EGFP
63 kDa

Figure 7. *Lv*TLR1 and *Lv*TLR2 in hemocytes is r*Lv*Prx4 target

(A) Toll-like receptor genes in the r*Lv*Prx4-injected shrimp were quantified using qRT-PCR. The *EF-1α* was employed as an internal control. Bar graphs demonstrate mean ± SD values and asterisk suggests statistically significant difference ($p < 0.05$).

(B) Co-localization of *Lv*Prx4 and *Lv*TLR1 or *Lv*TLR2 in HEK293T cells by immunofluorescence. The nucleus, *Lv*Prx4 and *Lv*TLR1 or *Lv*TLR2 are stained in blue (Hoechst 33342), red (Alexa Fluor 568) and green (EGFP tag) colors, respectively.

(C) Localization of r*Lv*Prx4 on *Lv*TLR1 or *Lv*TLR2-silencing hemocytes by immunofluorescence. The nucleus cytoplasmic membrane and r*Lv*Prx4 are visualized in blue (Hoechst 33342), red (CellBrite cytoplasmic membrane) and green (Alexa Fluor 488) colors, respectively.

(D) Pull down of *Lv*Prx4 with *Lv*TLR1 or *Lv*TLR2. The interacting proteins were separated by SDS-PAGE and analyzed by Western blotting with an anti-His antibody.

A pull-down assay was then performed to confirm the *Lv*Prx4/*Lv*TLR1 and *Lv*Prx4/*Lv*TLR2 interactions (Figure 7D). This assay revealed binding of *Lv*Prx4 to EGFP-tagged *Lv*TLR1 and *Lv*TLR2 (*Lv*TLR1_EGFP and *Lv*TLR2_EGFP) or *Lv*TLR1_LRR_EGFP and *Lv*TLR2_LRR_EGFP, confirming the *Lv*Prx4/*Lv*TLR1 and *Lv*Prx4/*Lv*TLR2 interactions. Cell lysates from HEK293T cells overexpressing *Lv*Prx4 with one of tested proteins including EGFP-tagged *Lv*TLR1 (*Lv*TLR1_EGFP), EGFP-tagged *Lv*TLR2 (*Lv*TLR2_EGFP), *Lv*TLR1_LRR_EGFP, and *Lv*TLR2_LRR_EGFP, or the control Renilla *Luciferase* (RL)_EGFP, were incubated with r*Lv*Prx4 and direct interactions were determined. The in-gel green fluorescence of all EGFP-tagged proteins except for that of the negative control, RL_EGFP, were detected, suggesting a direct interaction between the LRR domain of *Lv*TLR1 and *Lv*TLR2 as expected.

The downstream genes, *LvPEN4*, *LvALF AA-K*, and *LvVago5*, were then analyzed with respect to their expression in hemocyte when *LvTLR1* or *LvTLR2* were suppressed and r*Lv*Prx4 was introduced into shrimp. It was discovered that the presence of r*Lv*Prx4 expression of *LvPEN4* and *LvVago5* was not increased when *LvTLR1* and *LvTLR2* were suppressed. Nevertheless, knockdown of either *LvTLR1* or *LvTLR2* had no effect on increased expression of *LvALF AA-K* expression triggered by r*Lv*Prx4 (Figure 8). It was thus concluded that *Lv*Prx4 binds directly to *Lv*TLR1 and *Lv*TLR2 and induced expression of *LvPEN4* and *LvVago5*.

DISCUSSION

Exposure to above normal ambient temperature or non-lethal heat shock (NLHS) conditions can enhance resistance to pathogen infections in many organisms, especially aquatic animals although the exact mechanism has not been fully elucidated.[6,8–10] Heat-induced cell death from apoptosis and necrosis has been previously reported.[26–28] In principle, cell damage triggers release of endogenous DAMPs molecules.[29–31] It was previously demonstrated that NLHS increases the production of heat shock proteins (HSPs) as well as the biological immune responses.[10,11] In the present study, NLHS was confirmed to induce necrotic cell death and early apoptosis of shrimp hemocytes (Figure 1B).

Cellular damage caused by various stress types and stress-associated proteins such as HSPs have been demonstrated to induce cell death. Some HSPs present anti-apoptotic or pro-apoptotic properties; cytosolic HSP60 for instance, is an anti-apoptotic protein that binds to BAX protein in cardiac myocytes[32] and HSP70 is the other anti-apoptotic protein that inhibits translocation of BAX into the mitochondria as well as activation of initiator caspases.[33] Mitochondria HSP60 demonstrates pro-apoptotic properties because it binds to pro-caspase3 that results in induction of apoptosis.[34] Cell damage causes partial membrane permeabilization during early apoptosis, it also allows the release of DAMP proteins followed by the loss of membrane integrity during secondary necrosis. The released stress proteins promote innate immunity and adaptive immunity activation.[18] Heat stress can induce the production of reactive oxygen species (ROS), that trigger damage to lipids, DNA, RNA and proteins of the cell.[35] Short term heat shock on *Bradysia* adults can enhance lipid peroxidation and antioxidant enzyme activities.[36] In shrimp *P. vannamei*, temperature stress induced the expression of stressor biomarker and antioxidant enzymes in gills.[37] Nevertheless, antioxidant enzymes operating as DAMP proteins promoting NLHS-induced immune responses in shrimp remains unknown.

Peroxiredoxin (Prx), a family of antioxidant enzymes with peroxidase activity, have been previously reported as DAMPs in mammals. Prx regulates cytokine-induced peroxide levels and mediates signal transduction.[38] Prx also functions as a chaperone during heat stress to protect the host.[39] In the present study, five isoforms of *LvPrx* have been identified and examined for the expression pattern in various tissues and following NLHS treatment. As hemocytes are considered essential immune cells in shrimp immunity, *LvPrx4*, the most abundant and highly upregulated isoform following NLHS treatment in hemocytes, was selected for further characterization. *LvPrx4* was found to be highly expressed in heart, stomach, gills, muscle and

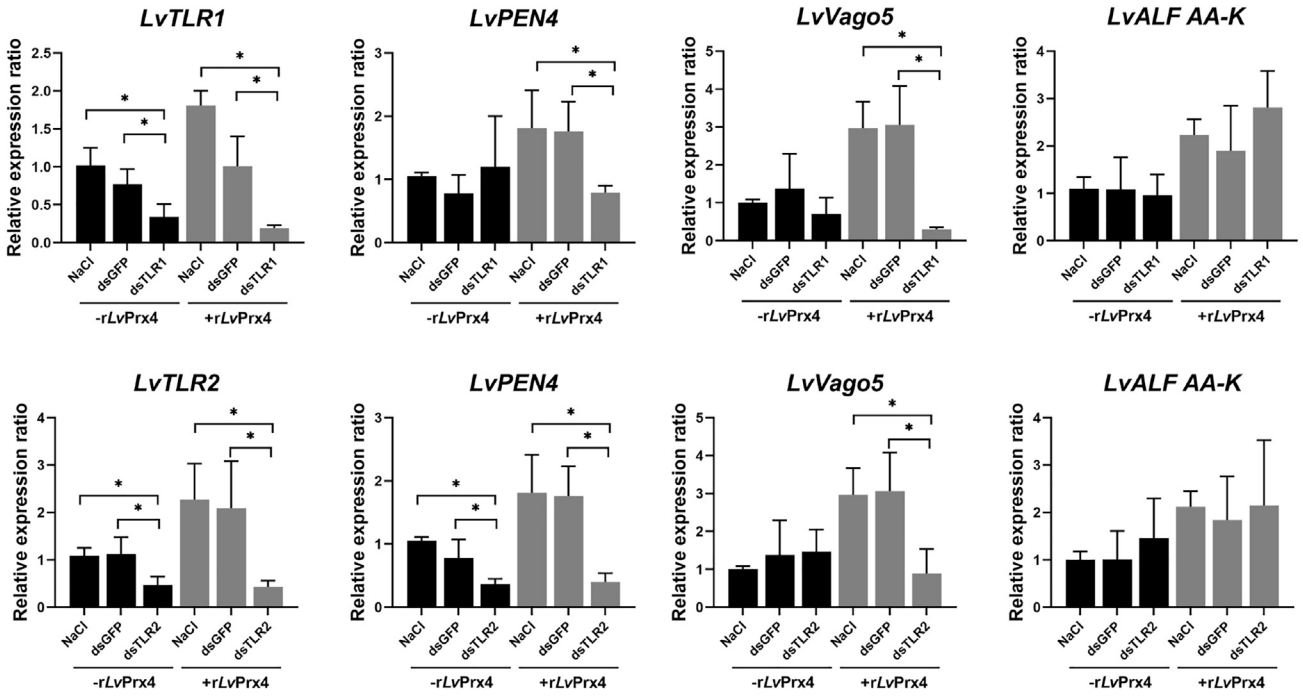

Figure 8. r*Lv*Prx4-induced immune response is mediated by *Lv*TLR1 and *Lv*TLR2 activation

LvTLR1 or *LvTLR2* were suppressed using specific dsRNA. Following a r*Lv*Prx4 injection, some immune-related genes were quantified with respect to their expression in hemocyte using qRT-PCR. *EF-1α* was employed as an internal control. Bar graphs show mean ± SD values and asterisk suggest a statistically significant difference ($p < 0.05$).

hemocytes. In *P. monodon*, *Prx4* presented elevated expression levels in heart, however, it could not be detected in muscle.[40] In addition, *Prx4* from *Fenneropenaeus chinensis*[41] and *P. clarkia*[42] were significantly expressed in the hepatopancreas, hemocytes and gill. Because of these different expression patterns, *Prx4* might differ depending on species.

With respect to the localization of Prx members, Prx1 and Prx2 are predominantly localized in the cytosol and transferred into the nucleus; Prx3 is localized only in the mitochondria; Prx4 can be found in the cytosol and the endoplasmic reticulum; Prx5 is localized in the cytosol and the mitochondria and Prx6 in the cytosol. Among the Prx members detected in fish, Prx1, Prx2 and Prx4 are secreted in the serum.[43] With respect to *LvPrx*s sequences, only *Lv*Prx4 contains the signal peptide, suggesting that most likely *Lv*Prx4 is the secreted protein. Following acute-NLHS treatment, *Lv*Prx4 protein and increased peroxidase activity was detected in hemolymph. *Lv*Prx4 was thus identified as an NLHS-induced DAMP based on its expression in hemocytes and the secretion into hemolymph as a reaction to NLHS treatment.

In the present study, it was discovered that r*Lv*Prx4 presents peroxidase activity and can decrease DNA damage as an antioxidant enzyme. *Lv*Prx4 in monomer and dimer forms was clearly detected in hemocyte following NLHS treatment (Figure 3B). It was hypothesized that upregulated *Lv*Prx4 under NLHS is a multifunctional protein that protects shrimp from oxidative stress and regulates intracellular transduction, as has been previously reported in many animals. Typical 2-Cys peroxiredoxins reduce hydrogen peroxide (H_2O_2) and associated oxidants through peroxidatic cysteine (Cp) associates with the resolving cysteine (Cr) on the second subunit of the dimer to form an intermolecular disulfide intermediate.[44] Various 2-cys peroxiredoxins are dual-function proteins that can serve as a peroxidase or a chaperone. Prxs in contrast, function as a chaperone for refolding misfolded proteins by reversible modifications in their quaternary structure that is defined by a toroid-shaped decamer made up of five catalytic dimers.[45] Conversion of peroxidase activity into molecular chaperone was induced by the overoxidation of active site cysteine and the production of oligomers.[46] When temperature was increased, mitochondrial 2-Cys peroxiredoxin in *Leishmania infantum* operates as peroxidase and chaperone to repair damaged or misfolded proteins.[47]

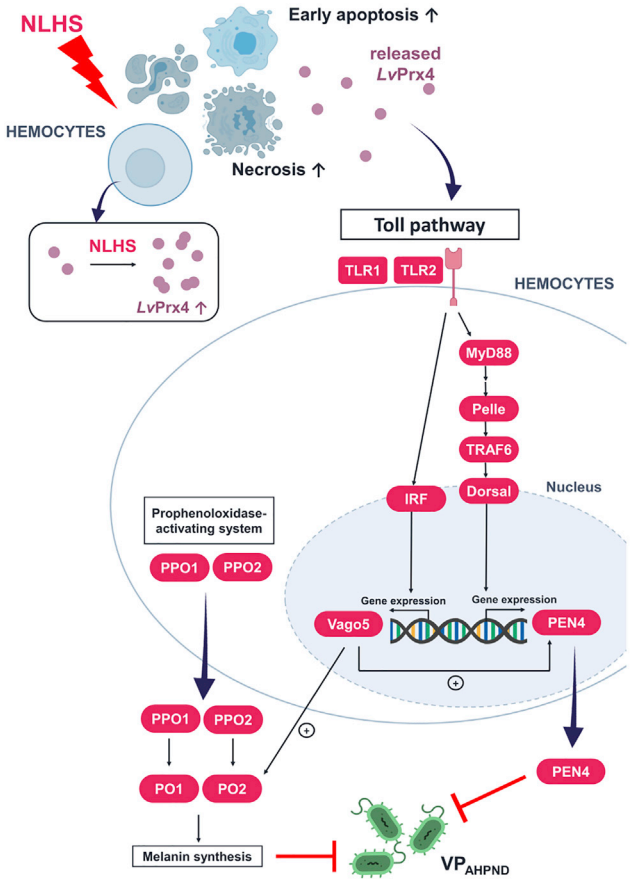

Figure 9. Summary schematic representation of NLHS-induced *Lv*Prx4 that enhances AHPND resistance in shrimp

Acute-NLHS treatment stimulates upregulation of *Lv*Prx4 that presents a peroxidase activity inhibiting DNA damage and chaperon activity in dimer form. Released *Lv*Prx4 plays a key role in increasing AHPND resistance in shrimp by inducing the prophenoloxidase-activating system and expression of immune-associated genes through *Lv*TLR1 and *Lv*TLR2-mediated signaling pathway.

Based on a previous report by our group,[11] NLHS has been demonstrated to promote immune responses such as the prophenoloxidase-activating system, hemocyte homeostasis, and antimicrobial peptide production, and these responses improve VP_{AHPND} resistance in *P. vannamei*. In the present study, it was discovered that silencing of *LvPrx4* triggered an increase in shrimp mortality following a challenge with VP_{AHPND}. r*Lv*Prx4 pre-injection in contrast, could prolong shrimp survival and decrease VP_{AHPND} copy number (Figure 4). Moreover, the melanin synthesis through the prophenoloxidase-activating system, the major innate defense mechanism was also activated on r*Lv*Prx4 injection (Figure 5). Furthermore, r*Lv*Prx4 injection may trigger immune signaling pathways by increasing the expression of genes coding for adaptor proteins as well as downstream genes of Toll and IRF/Vago pathways (Figure 6). The Toll pathway components and *LvDorsal* and *LvIRF* were significantly upregulated following r*Lv*Prx4 injection. *Lv*Dorsal controls the transcription of antimicrobial peptide penaeidin 4 (*Lv*PEN4)[48] in shrimp, that was found to be upregulated following r*Lv*Prx4 injection. With respect to the IRF/Vago pathway where the *Lv*IRF can promote the expression of the IFN-stimulated response element (ISRE)-containing promoter to trigger IFNs such as *Lv*Vagos,[23,24] increased expression of *Lv*IRF and *Lv*Vago5 following r*Lv*Prx4 injection was demonstrated, indicating an immune modulating role for *Lv*Prx4. *Lv*Vago5 itself has been demonstrated to participate in antibacterial response through regulation of the Toll/IMD pathway/*Lv*PEN4, JAK/STAT pathway and prophenoloxidase-activating system.[25] NLHS and *Lv*Prx4 might thus trigger the synergistic impact on significant immune activation and VP_{AHPND} resistance.

Increasing evidence thus demonstrates that peroxiredoxins act as DAMP and activate the immune response though Toll pathway. The recombinant peroxiredoxin 1 protein of *Toxoplasma gondii*, a

protozoan parasite that infects the warm-blooded animals, can induce activation of NF-kB, IL-6 production and interferon-gamma production in mouse.[49] In humans, Prx2 has been shown to interact with Toll-like receptor (TLR) 4 following traumatic brain injury and then induced the expression of the proinflammatory response.[19] Extracellular Prx5 has also been shown to bind to TLR4 receptor following macrophage modulating proinflammatory cytokine release and cell stiffening.[32] The C-terminal domain of peroxiredoxin in anaerobic parasitic amoebozoan, *Entamoeba histolytica*, also triggered TLR4-dependent activation of NLRP3 inflammasome in macrophages through caspase-1-dependent canonical pathway.[50] The mechanism of immune response activation following r*Lv*Prx4 injection may involve the regulation of antimicrobial peptides and interferons through Toll pathway as the presented data indicate that r*Lv*Prx4 injection could not promote the expression of *LvPEN4* and *LvVago5* when *LvTLR1* or *LvTLR2* was inhibited (Figure 8). Of interest, *LvALF AA-K* was overexpressed in r*Lv*Prx4-injected shrimp and was upregulated despite silencing of the toll-like receptor. Previous studies report the relationship between the prophenoloxidase-activating system and the AMPs synthesis.[51,52] Upregulation of *LvPPO1* and *LvPPO2* might thus be correlated with the expression of *LvALF AA-K*.

In summary, following acute-NLHS treatment, necrotic and early apoptotic cell death in hemocytes was significantly increased, resulting in release of intracellular molecules that stimulate the immune response. Among the NLHS-responsive *LvPrxs*, *LvPrx4* function has been characterized. *Lv*Prx4 was significantly increased in hemocytes and released into hemolymph following acute-NLHS treatment where increased peroxidase activity was also observed. The r*Lv*Prx4, exhibiting peroxidase activity can prevent DNA damage *in vitro* and presents an important role in enhancing AHPND resistance in shrimp by stimulating the prophenoloxidase-activating system, *LvPEN4* and *LvVago5* expression via TLR1-and TLR2-associated signaling pathway (Figure 9). Based on the above, the dual roles of *Lv*Prx4 are proposed as an antioxidant enzyme and as a danger signal that stimulates shrimp innate immunity. *Lv*Prx4 thus promotes shrimp resistance to VP_{AHPND} infection enhancement, making it a decent immunostimulant candidate in shrimp aquaculture.

Limitations of the study

The current study demonstrates that *Lv*Prx4 modulates *Lv*TLR mediated signaling pathway, resulting in the enhanced gene expression of antimicrobial peptides and interferon-like protein. However, the proPO system activation mechanism by *Lv*Prx4 is still elusive.

STAR★METHODS

Detailed methods are provided in the online version of this paper and include the following:

- KEY RESOURCES TABLE
- RESOURCE AVAILABILITY
  - Lead contact
  - Materials availability
  - Data and code availability
- EXPERIMENTAL MODEL AND SUBJECT DETAILS
  - Animals
  - Challenge experiments
- METHOD DETAILS
  - Hemocyte necrosis and apoptosis after acute non-lethal heat shock (acute-NLHS) treatment
  - Expression analysis of genes after acute-NLHS treatment
  - Sequence analysis
  - Tissue distribution of *LvPrxs*
  - Recombinant protein expression and purification
  - Western blot analysis of acute-NLHS treated-shrimp hemocytes and hemolymph
  - *Lv*Prx4 localization on acute-NLHS treated-shrimp hemocytes by immunofluorescence
  - Peroxidase activity assay
  - Metal-catalyzed oxidation (MCO) assay
  - Cumulative mortality assay on *LvPrx4* silenced- or r*Lv*Prx4 injected-shrimp
  - Bacterial counting and binary Pir toxin copy number quantification
  - Determination of H_2O_2 level in the VP_{AHPND}-challenged shrimp
  - Effect of the r*Lv*Prx4-injected shrimp on the expression of the immune-related genes in hemocyte and on PO activity in hemolymph

- Co-localization of r*Lv*Prx4 and *Lv*TLR
- Localization of r*Lv*Prx4 on TLR-silencing hemocytes by immunofluorescence
- *In vitro* pull-down of *Lv*Prx4 with *Lv*TLR1 and 2
- Identification of r*Lv*Prx4-induced pathway using RNAi interference

● QUANTIFICATION AND STATISTICAL ANALYSIS

SUPPLEMENTAL INFORMATION

Supplemental information can be found online at https://doi.org/10.1016/j.isci.2022.105793.

ACKNOWLEDGMENTS

This research was funded by Thailand Science Research and Innovation Fund Chulalongkorn University (CU_FRB65_food (10)118_23_48). The student fellowships to S.W. from theRoyal Golden Jubilee Ph.D. program, National Research Council of Thailand (Grant No. PHD/0026/2561) and the 90th Anniversary of Chulalongkorn University Fund, Chulalongkorn University (Grant No. GCUGR1125633058D No. 1–58) are appreciated. We also gratefully acknowledge an additional support from the Ratchadaphisek Somphot Endowment Fund, Chulalongkorn University to the Center of Excellence for Molecular Biology and Genomics of Shrimp. The funders had no role in study design, data collection and interpretation, or the decision to submit the work for publication.

AUTHOR CONTRIBUTIONS

K.S. contributed conceptualization, supervision, and funding acquisition. T.K. helped supervise the experiment. S.W. and K.S. designed the experiments. S.W. and P.J. conducted the experiments and analyzed the data. S.W. and K.S. wrote, reviewed, and edited the manuscript. All authors discussed the results, provided critical feedback and helped shape the research, analysis, and manuscript. All authors approved the final version of the manuscript.

DECLARATION OF INTERESTS

The authors declare no competing interests.

INCLUSION AND DIVERSITY

We support inclusive, diverse, and equitable conduct of research.

Received: August 9, 2022
Revised: October 1, 2022
Accepted: December 8, 2022
Published: January 20, 2023

REFERENCES

1. Tassanakajon, A., Rimphanitchayakit, V., Visetnan, S., Amparyup, P., Somboonwiwat, K., Charoensapsri, W., and Tang, S. (2018). Shrimp humoral responses against pathogens: antimicrobial peptides and melanization. Dev. Comp. Immunol. *80*, 81–93.

2. Bianchi, M.E. (2007). DAMPs, PAMPs and alarmins: all we need to know about danger. J. Leukoc. Biol. *81*, 1–5.

3. Harris, H.E., and Raucci, A. (2006). Alarmin (g) news about danger: workshop on innate danger signals and HMGB1. EMBO Rep. *7*, 774–778.

4. Zelenay, S., and e Sousa, C.R. (2013). Adaptive immunity after cell death. Trends Immunol. *34*, 329–335.

5. Zhang, X., Yuan, J., Sun, Y., Li, S., Gao, Y., Yu, Y., Liu, C., Wang, Q., Lv, X., and Zhang, X. (2019). Penaeid shrimp genome provides insights into benthic adaptation and frequent molting. Nat. Commun. *10*, 1–14.

6. Sung, Y.Y., Van Damme, E.J., Sorgeloos, P., and Bossier, P. (2007). Non-lethal heat shock protects gnotobiotic *Artemia franciscana* larvae against virulent Vibrios. Fish Shellfish Immunol. *22*, 318–326.

7. Norouzitallab, P., Baruah, K., Muthappa, D.M., and Bossier, P. (2015). Non-lethal heat shock induces HSP70 and HMGB1 protein production sequentially to protect *Artemia franciscana* against *Vibrio campbellii*. Fish Shellfish Immunol. *42*, 395–399.

8. de la Vega, E., Hall, M.R., Degnan, B.M., and Wilson, K.J. (2006). Short-term hyperthermic treatment of *Penaeus monodon* increases expression of heat shock protein 70 (HSP70) and reduces replication of gill associated virus (GAV). Aquaculture *253*, 82–90.

9. Aleng, N.A., Sung, Y.Y., MacRae, T.H., and Abd Wahid, M.E. (2015). Non-lethal heat shock of the Asian green mussel, *Perna viridis*, promotes Hsp70 synthesis, induces thermotolerance and protects against Vibrio infection. PLoS One *10*, e0135603.

10. Junprung, W., Supungul, P., and Tassanakajon, A. (2017). HSP70 and HSP90 are involved in shrimp *Penaeus vannamei* tolerance to AHPND-causing strain of *Vibrio parahaemolyticus* after non-lethal heat shock. Fish Shellfish Immunol. *60*, 237–246.

11. Boonchuen, P., Maralit, B.A., Jaree, P., Tassanakajon, A., and Somboonwiwat, K. (2020). MicroRNA and mRNA interactions coordinate the immune response in non-lethal heat stressed *Litopenaeus vannamei* against AHPND-causing *Vibrio parahaemolyticus*. Sci. Rep. *10*, 1–15.

12. He, Y., Li, S., Tang, D., Peng, Y., Meng, J., Peng, S., Deng, Z., Qiu, S., Liao, X., and Chen, H. (2019). Circulating Peroxiredoxin-1 is a novel damage-associated molecular pattern and aggravates acute liver injury via promoting inflammation. Free Radic. Biol. Med. *137*, 24–36.

13. Ooboshi, H., and Shichita, T. (2016). DAMPs (damage-associated molecular patterns) and inflammation. Nihon Rinsho *74*, 573–578.

14. Gallucci, S., and Matzinger, P. (2001). Danger signals: SOS to the immune system. Curr. Opin. Immunol. *13*, 114–119.

15. Salzano, S., Checconi, P., Hanschmann, E.-M., Lillig, C.H., Bowler, L.D., Chan, P., Vaudry, D., Mengozzi, M., Coppo, L., and Sacre, S. (2014). Linkage of inflammation and oxidative stress via release of glutathionylated peroxiredoxin-2, which acts as a danger signal. Proc. Natl. Acad. Sci. USA *111*, 12157–12162.

16. Morales-Lange, B., González-Aravena, M., Font, A., Guzmán, F., and Mercado, L. (2018). Detection of peroxiredoxin-like protein in Antarctic sea urchin (*Sterechinus neumayeri*) under heat stress and induced with pathogen-associated molecular pattern from Vibrio anguillarum. Polar Biol. *41*, 2065–2073.

17. Duan, Y., Liu, P., Li, J., Li, J., Gao, B., and Chen, P. (2013). cDNA cloning, characterization and expression analysis of peroxiredoxin 5 gene in the ridgetail white prawn *Exopalaemon carinicauda*. Mol. Biol. Rep. *40*, 6569–6577.

18. Wickman, G., Julian, L., Mardilovich, K., Schumacher, S., Munro, J., Rath, N., Zander, S.A., Mleczak, A., Sumpton, D., and Morrice, N. (2013). Blebs produced by actin–myosin contraction during apoptosis release damage-associated molecular pattern proteins before secondary necrosis occurs. Cell Death Differ. *20*, 1293–1305.

19. Lu, Y., Zhang, X.-S., Zhang, Z.-H., Zhou, X.-M., Gao, Y.-Y., Liu, G.-J., Wang, H., Wu, L.-Y., Li, W., and Hang, C.-H. (2018). Peroxiredoxin 2 activates microglia by interacting with Toll-like receptor 4 after subarachnoid hemorrhage. J. Neuroinflammation *15*, 1–10.

20. Knoops, B., Argyropoulou, V., Becker, S., Ferté, L., and Kuznetsova, O. (2016). Multiple roles of peroxiredoxins in inflammation. Mol. Cell. *39*, 60.

21. Shichita, T., Hasegawa, E., Kimura, A., Morita, R., Sakaguchi, R., Takada, I., Sekiya, T., Ooboshi, H., Kitazono, T., and Yanagawa, T. (2012). Peroxiredoxin family proteins are key initiators of post-ischemic inflammation in the brain. Nat. Med. *18*, 911–917.

22. Charoensapsri, W., Amparyup, P., Suriyachan, C., and Tassanakajon, A. (2014). Melanization reaction products of shrimp display antimicrobial properties against their major bacterial and fungal pathogens. Dev. Comp. Immunol. *47*, 150–159.

23. Li, C., Li, H., Chen, Y., Chen, Y., Wang, S., Weng, S.-P., Xu, X., and He, J. (2015). Activation of Vago by interferon regulatory factor (IRF) suggests an interferon system-like antiviral mechanism in shrimp. Sci. Rep. *5*, 1–13.

24. Li, H., Fu, Q., Wang, S., Chen, R., Jiang, X., Zhu, P., He, J., and Li, C. (2020). TNF-Receptor-Associated factor 3 in *Litopenaeus vannamei*restricts white spot syndrome virus infection through the IRF-vago antiviral pathway. Front. Immunol. *11*, 2110.

25. Boonchuen, P., Sakhor, H., Jaree, P., and Somboonwiwat, K. (2022). Shrimp Vago5 activates an innate immune defense upon bacterial infection. Fish Shellfish Immunol. *120*, 122–132.

26. Li, S., Chien, S., and Brånemark, P.I. (1999). Heat shock-induced necrosis and apoptosis in osteoblasts. J. Orthop. Res. *17*, 891–899.

27. Thompson, S.M., Callstrom, M.R., Butters, K.A., Knudsen, B., Grande, J.P., Roberts, L.R., and Woodrum, D.A. (2014). Heat stress induced cell death mechanisms in hepatocytes and hepatocellular carcinoma: in vitro and in vivo study. Laser Surg. Med. *46*, 290–301.

28. Janko, C., Munoz, L., Chaurio, R., Maueröder, C., Berens, C., Lauber, K., and Herrmann, M. (2013). Navigation to the graveyard-induction of various pathways of necrosis and their classification by flow cytometry. In Necrosis (Springer), pp. 3–15.

29. Srikrishna, G., and Freeze, H.H. (2009). Endogenous damage-associated molecular pattern molecules at the crossroads of inflammation and cancer. Neoplasia *11*, 615–628.

30. Roh, J.S., and Sohn, D.H. (2018). Damage-associated molecular patterns in inflammatory diseases. Immune Netw. *18*. https://doi.org/10.4110/in.2018.18.e27.

31. Schaefer, L. (2014). Complexity of danger: the diverse nature of damage-associated molecular patterns. J. Biol. Chem. *289*, 35237–35245.

32. Kirchhoff, S., Gupta, S., and Knowlton, A.A. (2002). Cytosolic heat shock protein 60, apoptosis, and myocardial injury. Circulation *105*, 2899–2904.

33. Arya, R., Mallik, M., and Lakhotia, S.C. (2007). Heat shock genes—integrating cell survival and death. J. Biosci. *32*, 595–610.

34. Samali, A., Cai, J., Zhivotovsky, B., Jones, D.P., and Orrenius, S. (1999). Presence of a pre-apoptotic complex of pro-caspase-3, Hsp60 and Hsp10 in the mitochondrial fraction of jurkat cells. EMBO J. *18*, 2040–2048.

35. Feng, J., Zhang, M., Zheng, S., Xie, P., and Ma, A. (2008). Effects of high temperature on multiple parameters of broilers *in vitro* and *in vivo*. Poultry Sci. *87*, 2133–2139.

36. Zhu, G., Xue, M., Luo, Y., Ji, G., Liu, F., Zhao, H., and Sun, X. (2017). Effects of short-term heat shock and physiological responses to heat stress in two Bradysia adults, *Bradysia odoriphaga* and *Bradysia difformis*. Sci. Rep. *7*, 1–11.

37. Zhou, J., Wang, L., Xin, Y., Wang, W.-N., He, W.-Y., Wang, A.-L., and Liu, Y. (2010). Effect of temperature on antioxidant enzyme gene expression and stress protein response in white shrimp, *Litopenaeus vannamei*. J. Therm. Biol. *35*, 284–289.

38. Bolduc, J., Koruza, K., Luo, T., Pueyo, J.M., Vo, T.N., Ezeriņa, D., and Messens, J. (2021). Peroxiredoxins wear many hats: factors that fashion their peroxide sensing personalities. Redox Biol. *42*, 101959.

39. Teixeira, F., Tse, E., Castro, H., Makepeace, K.A., Meinen, B.A., Borchers, C.H., Poole, L.B., Bardwell, J.C., Tomás, A.M., and Southworth, D.R. (2019). Chaperone activation and client binding of a 2-cysteine peroxiredoxin. Nat. Commun. *10*, 1–14.

40. Qiu, L., Ma, Z., Jiang, S., Wang, W., Zhou, F., Huang, J., Li, J., and Yang, Q. (2010). Molecular cloning and mRNA expression of peroxiredoxin gene in black tiger shrimp (*Penaeus monodon*). Mol. Biol. Rep. *37*, 2821–2827.

41. Zhang, Q., Huang, J., Li, F., Liu, S., Liu, Q., Wei, J., Liang, G., and Xiang, J. (2014). Molecular characterization, immune response against white spot syndrome virus infection of peroxiredoxin 4 in *Fenneropenaeus chinensis* and its antioxidant activity. Fish Shellfish Immunol. *37*, 38–45.

42. Dai, L.-S., Yu, X.-M., Abbas, M.N., Li, C.-S., Chu, S.-H., Kausar, S., and Wang, T.-T. (2018). Essential role of the peroxiredoxin 4 in *Procambarus clarkii* antioxidant defense and immune responses. Fish Shellfish Immunol. *75*, 216–222.

43. Valero, Y., Martínez-Morcillo, F.J., Esteban, M.Á., Chaves-Pozo, E., and Cuesta, A. (2015). Fish peroxiredoxins and their role in immunity. Biology *4*, 860–880.

44. Nicolussi, A., D'inzeo, S., Capalbo, C., Giannini, G., and Coppa, A. (2017). The role of peroxiredoxins in cancer. Mol. Clin. Oncol. *6*, 139–153.

45. Wang, X., Wang, L., Wang, X.e., Sun, F., and Wang, C.-c. (2012). Structural insights into the peroxidase activity and inactivation of human peroxiredoxin 4. Biochem. J. *441*, 113–118.

46. Teixeira, F., Castro, H., Cruz, T., Tse, E., Koldewey, P., Southworth, D.R., Tomás, A.M., and Jakob, U. (2015). Mitochondrial peroxiredoxin functions as crucial chaperone reservoir in Leishmania infantum. Proc. Natl. Acad. Sci. USA *112*, E616–E624.

47. Castro, H., Teixeira, F., Romao, S., Santos, M., Cruz, T., Flórido, M., Appelberg, R., Oliveira, P., Ferreira-da-Silva, F., and Tomás, A.M. (2011). Leishmania mitochondrial peroxiredoxin plays a crucial peroxidase-unrelated role during infection: insight into its novel chaperone activity. PLoS Pathog. *7*, e1002325.

48. Huang, X.-D., Yin, Z.-X., Jia, X.-t., Liang, J.-p., Ai, H.-S., Yang, L.-S., Liu, X., Wang, P.-H., Li, S.-d., and Weng, S.-P. (2010). Identification and functional study of a shrimp Dorsal

homologue. Dev. Comp. Immunol. *34*, 107–113.

49. Fereig, R.M., Kuroda, Y., Terkawi, M.A., Mahmoud, M.E., and Nishikawa, Y. (2017). Immunization with Toxoplasma gondii peroxiredoxin 1 induces protective immunity against toxoplasmosis in mice. PLoS One *12*, e0176324.

50. Li, X., Feng, M., Zhao, Y., Zhang, Y., Zhou, R., Zhou, H., Pang, Z., Tachibana, H., and Cheng, X. (2021). A novel TLR4-binding domain of peroxiredoxin from Entamoeba histolytica triggers NLRP3 inflammasome activation in macrophages. Front. Immunol. *12*.

51. Amparyup, P., Charoensapsri, W., and Tassanakajon, A. (2013). Prophenoloxidase system and its role in shrimp immune responses against major pathogens. Fish Shellfish Immunol. *34*, 990–1001.

52. Fagutao, F.F., Koyama, T., Kaizu, A., Saito-Taki, T., Kondo, H., Aoki, T., and Hirono, I. (2009). Increased bacterial load in shrimp hemolymph in the absence of prophenoloxidase. FEBS J. *276*, 5298–5306.

53. Benson, D.A., Cavanaugh, M., Clark, K., Karsch-Mizrachi, I., Ostell, J., Pruitt, K.D., and Sayers, E.W. (2018). GenBank. Nucleic Acids Res. *46*, D41–D47.

54. Afgan, E., Baker, D., Batut, B., Van Den Beek, M., Bouvier, D., Čech, M., Chilton, J., Clements, D., Coraor, N., and Grüning, B.A. (2018). The Galaxy platform for accessible, reproducible and collaborative biomedical analyses: 2018 update. Nucleic Acids Res. *46*, W537–W544.

55. Duvaud, S., Gabella, C., Lisacek, F., Stockinger, H., Ioannidis, V., and Durinx, C. (2021). Expasy, the Swiss bioinformatics resource portal, as designed by its users. Nucleic Acids Res. *49*, W216–W227.

56. Kumar, S., Stecher, G., Li, M., Knyaz, C., and Tamura, K. (2018). Mega X: molecular evolutionary genetics analysis across computing platforms. Mol. Biol. Evol. *35*, 1547.

57. Almagro Armenteros, J.J., Tsirigos, K.D., Sønderby, C.K., Petersen, T.N., Winther, O., Brunak, S., von Heijne, G., and Nielsen, H. (2019). SignalP 5.0 improves signal peptide predictions using deep neural networks. Nat. Biotechnol. *37*, 420–423.

58. Lu, S., Wang, J., Chitsaz, F., Derbyshire, M.K., Geer, R.C., Gonzales, N.R., Gwadz, M., Hurwitz, D.I., Marchler, G.H., and Song, J.S. (2020). CDD/SPARCLE: the conserved domain database in 2020. Nucleic Acids Res. *48*, D265–D268.

59. Waterhouse, A., Bertoni, M., Bienert, S., Studer, G., Tauriello, G., Gumienny, R., Heer, F.T., de Beer, T.A.P., Rempfer, C., and Bordoli, L. (2018). SWISS-MODEL: homology modelling of protein structures and complexes. Nucleic Acids Res. *46*, W296–W303.

60. Posiri, P., Ongvarrasopone, C., and Panyim, S. (2013). A simple one-step method for producing dsRNA from E. coli to inhibit shrimp virus replication. J. Virol Methods *188*, 64–69.

STAR★METHODS

KEY RESOURCES TABLE

REAGENT or RESOURCE	SOURCE	IDENTIFIER
Antibodies		
mouse anti-His antibody	Abcam	Cat# ab18184; RRID: AB_444306
mouse anti-GST antibody	Abcam	Cat# EPR4236; RRID: AB_10861266
goat anti-mouse HRP	Abcam	Cat# ab6789; RRID: AB_955439
goat anti-rabbit HRP	Abcam	Cat# ab6721; RRID: AB_95544
goat anti-rabbit Alexa Fluor 568	Thermo Fisher	Cat # A78955; RRID: AB_2925778
rabbit anti-*Lv*Prx4	This paper	N/A
Bacterial and virus strains		
Vibrio parahaemolyticus	Lab isolated strain	N/A
Biological samples		
shrimp *Penaeus vannamei*	Charoen Pokphand Foods PCL, Thailand	N/A
Chemicals, peptides, and recombinant proteins		
BD Bacto™ Tryptic Soy Broth (Soybean-Casein Digest Medium)	Fisher Scientific	Cat# DF0370-17-3
BD Difco™ Dehydrated Culture Media: TCBS Agar	Fisher Scientific	Cat# DF0650-17-4
GENEzol™ reagent	Geneaid	Cat# GZR100
DNase I	Thermo Fisher	Cat# EN0521
Luna® Universal qPCR Master Mix	New England Biolabs	Cat# M3003L
L-DOPA	Sigma	Cat# 59-92-7
Critical commercial assays		
realtime-Glo™ annexin V apoptosis and necrosis assay	Promaga	Cat# JA1011
RevertAid™ First Strand cDNA Synthesis Kit	Thermo Fisher	Cat# K1621
Experimental models: Cell lines		
Human HEK-293T cell line	Abcam	Cat# ab255449
Oligonucleotides		
Primer for RT-PCR and qRT-PCR, see Table S1	This paper	N/A
Primer for RNAi, see Table S1	This paper	N/A
Primer for protein expression, see Table S1	This paper	N/A
Software and algorithms		
GraphPad Prism Version 9 for Windows	GraphPad Software	https://www.graphpad.com/
Adobe Photoshop	Adobe	https://www.adobe.com/

RESOURCE AVAILABILITY

Lead contact

Further information and requests for resources and reagents should be directed to and will be fulfilled by the Lead Contact, Kunlaya Somboonwiwat (Kunlaya.S@chula.ac.th)

Materials availability

This study did not generate new unique reagents.

Data and code availability

- The raw sequencing data and all other data used for this study will be shared upon reasonable request from the lead contact.

- This paper does not report original code.
- Any additional information required to reanalyze the data reported in this paper is available from the lead contact upon request.

EXPERIMENTAL MODEL AND SUBJECT DETAILS

Animals

Healthy shrimp *P. vannamei* with an average weight 3–5 g were obtained from Charoen Pokphand Foods PCL, Thailand. VP_{AHPND} were isolated from shrimp farm in Chanthaburi provinces in Thailand. This project was conducted according to the animal use protocol number 1923018 approved by the Chulalongkorn University Animal Care and Use Committee (CU-ACUC) and the biosafety was approved by the Institutional Biosafety Committee of Chulalongkorn University (SCCU-IBC-0010/2018).

Challenge experiments

VP_{AHPND} were grown overnight at 30 °C in tryptic soy agar plates (TSA) supplemented with 1.5% NaCl and inoculated into tryptic soy broth (TSB) containing 1.5% NaCl at 30 °C, 16 h and 250 rpm. Then, the starter culture was inoculated 1:100 into TSB with 1.5% NaCl and incubated at 30 °C and 250 rpm until the OD_{600} reached 2.0 (approximately 10^8 CFU/mL). Shrimp were challenged at a final concentration 5×10^5 CFU/mL (LD_{50} = 48 hpi) by immersion.

METHOD DETAILS

Hemocyte necrosis and apoptosis after acute non-lethal heat shock (acute-NLHS) treatment

In vitro assay, shrimp hemolymph was drawn out using a sterile syringe with an equal volume of anticoagulant (27 mM sodium citrate, 336 mM NaCl, 115 mM glucose and 9 mM EDTA, pH 5.6). Shrimp hemocytes were collected by centrifugation at 800×g, 4 °C for 15 min. Cells were resuspended in L15 medium and added 50 μL of 2×10^6 cells/ml to 96-well plate. Hemocytes were incubated at 36°C for 30 min. Necrosis and apoptosis were evaluated using realtime-Glo annexin V apoptosis and necrosis assay (Promaga).

In vivo assay, shrimp acclimated at 28°C and were separated into 2 groups of non-heated control and heated groups. In the acute-NLHS group, shrimp were incubated at 36°C for 30 min and then transferred immediately back to 28°C for recovery. After 3 h recovery, hemolymph of three individuals was drawn out and hemocytes and collected by centrifugation. About 10,000 cells were stained with Annexin-V and PI in binding buffer. After washing with PBS, the hemocyte death rate was analyzed by flow cytometer (BD Accuri™ C6 Plus, Biosciences).

Expression analysis of genes after acute-NLHS treatment

Shrimp were exposed to acute-NLHS treatment as described above. After 3, 48 and 72 h recovery, hemocytes of three individuals were pooled and collected to the total RNA extraction using GENEzol reagent (Geneaid) and the contaminated genomic DNA was eliminated by DNase I (Thermo Fisher). The quality and quantity of the total RNA was analyzed by NanoDrop Spectophotometer and 1.2% agarose gel electrophoresis. Then, cDNA was synthesized using RevertAid First Strand cDNA Synthesis Kit (Thermo Fisher). The expression level was determined by qRT-PCR. Reactions was performed in CFX96 Touch Real-Time PCR Detection System (Bio-Rad) using Luna Universal qPCR Master Mix (New England Biolabs) with specific primers (Table S1). The reaction condition was performed with an initial denaturation at 95°C for 60 s, followed by 40 cycles of denaturation at 95°C for 15 s and extension at 60°C for 30 s. Melting curve analysis was performed from 60 to 95°C with continuous fluorescent reading every 0.5°C. Relative expression of each gene was analyzed using the *EF-1α* gene as a control gene. The statistical significance was tested at $p < 0.05$.

Sequence analysis

All Prx sequences were obtained from shrimp *P. vannamei* genomic database[5] and the GenBank server.[53] The Fasta and BLAST tools from galaxy services of the National Center for Genome Analysis Support were used for the sequence analysis.[54] Protein translation was achieved using ExPASy.[55] Phylogenetic analysis was carried out the maximum likelihood algorithm employing the Poisson correction method with 1,000 bootstrap re-sampling in MEGA-X software.[56] Prediction of the signal peptide at N-terminus of *Lv*Prxs amino acid sequences were analyzed with SignalP 5.0 [57] and the conserved domains (CD) was identified

by CD-search in NCBI.[58] The model structure of *Lv*Prx4 was predicted by SWISS-MODEL[59] based on the published crystal structure PDB 3TKR.

Tissue distribution of *LvPrxs*

Healthy shrimp were dissected and tissues including hemocytes, heart, hepatopancreas, gills, muscle, intestines, stomach and lymphoid were collected. Semi-quantitative RT-PCR was performed by using *LvPrxs* gene specific primers (Table S1) using cDNA, extracted from various tissues of healthy shrimp as template. The PCR products were analyzed by 1.2% agarose gel electrophoresis. The relative expression was determined using elongation factor-1α (*EF-1α*) as an internal control.

Recombinant protein expression and purification

The coding region of *LvPrx4* were amplified using the specific primer pair containing restriction sites for NcoI and NdeI (Table S1). The PCR product digested with the corresponding restriction enzymes was cloned into the vector pET19b. After sequence confirmation, the recombinant plasmid was transformed into the expression host *E. coli* BL21(DE). The pGEX vector harboring GST coding sequence was transformed into *E. coli* BL21(DE) to produce GST control protein. The single colony of *E. coli* harboring the expression plasmids was cultured and induced for recombinant protein expression using 1 mM IPTG. Then, the cells were collected and the overexpression of the recombinant *Lv*Prx4 (r*Lv*Prx4) and GST (rGST) was verified by 12.5% (w/v) SDS-PAGE. Western blot using anti-His or anti-GST antibody (Abcam), respectively. followed by the appropriate secondary antibody incubation and chemiluminescent detection was also performed.

The overexpressed r*Lv*Prx4 was further purified using Ni-NTA column (GE healthcare). The overexpressed rGST was further purified using Glutathione agarose resin (Gold Biotechology). The purified proteins were dialyzed against 20 mM Tris-Cl pH 8.0 and kept at −80°C until used. The protein concentration was determined using Bradford reagent (Bio-rad).

Western blot analysis of acute-NLHS treated-shrimp hemocytes and hemolymph

Hemolymph were drawn out from three shrimp using a sterile syringe with an equal volume of anticoagulant and centrifugated to separate the hemocytes. After washing twice with 1×PBS pH 7.4, the hemocytes were homogenized in 1×PBS pH 7.4. Cell-free hemolymph was loaded onto a Blue-Sepharose column pre-equilibrate with 50 mM Tris pH 8.0 and the flow-through fraction was precipitated with cold acetone: methanol (3:1 (%v/v)) at −20°C for 3 h and centrifugated at 14,000×g for 10 minat 4 °C. The pellet was washed with cold acetone and solubilized in rehydration buffer (8 M urea, 2 M thiourea, 4% (%w/v) CHAPS and 1 mM PMSF). The total protein was measured using Bradford assay. Hemocyte lysate and partial purified hemolymph (50 μg) was separated on 12.5% (w/v) SDS-PAGE and Western blot was performed using a rabbit polyclonal antibody specific to *Lv*Prx4 at 1:500 dilution and the 1:10,000 diluted HRP conjugated goat anti-mouse IgG which was then detected by chemiluminescence.

*Lv*Prx4 localization on acute-NLHS treated-shrimp hemocytes by immunofluorescence

Acute-NLHS treated-shrimp hemocytes were collected after 72 h recovery by centrifugation at 800×g, 15 min, 4°C. The cell pellet was fixed with 4% (w/v) paraformaldehyde pH 6.0 and washed with 1×PBS pH 7.4 buffer. The fixed cells were kept at 4°C until use. Cells (4×10^5 cells/ml) were fixed onto the poly-L-lysine (Sigma) coated-coverslips overnight and washed with washing buffer (0.02% Triton X-100 in 1×PBS pH 7.4). Cell membrane was stained with Cell Brite cytoplasmic membrane dye (Biotium) for 10 minat the ratio of 1:200 in blocking buffer (0.02% Triton X-100, 10% FBS and 1% BSA in 1×PBS pH 7.4) and washed with washing buffer followed by permeabilizing with 1×PBS pH 7.4 containing 0.2% gelatin, 1% BSA and 0.02%Triton X-100 for 30 min. Then, cells were washed again and blocked with blocking buffer for 2 h. After washing, cells were probed with a 1:500 rabbit polyclonal anti-*Lv*Prx4 antibody in blocking buffer at 4°C, overnight followed by washing and addition of an anti-rabbit secondary antibody conjugated with Alexa Fluor 488 at ratio of 1:1,000 at room temperature for 2 h. The nuclei were stained with Hoechst 33,342 at ratio of 1:5,000 (Thermo Fisher). The cells on coverslips were mounted with EverBrite Mounting Medium (Biotium) and sealed on glass slides. Fluorescence images were detected with LSM 900 laser scanning confocal microscope (Carl Zeiss).

Peroxidase activity assay

The peroxidase activity of the r*Lv*Prx4 and of acute NLHS-treated shrimp hemolymph were assayed by mixing samples with 100 mM phosphate buffer pH 6.0, then added 17 μL of freshly prepared solution of 50 mg/mL pyrogallol (Merck) and 30% (w/w) hydrogen peroxide. Absorbance at 420 nm was monitored.

Metal-catalyzed oxidation (MCO) assay

The plasmid DNA (pEGFP-N1, 300 ng) was incubated with reaction mixture containing 5 mM DTT, 20 μM $FeCl_3$ and the absence or presence of r*Lv*Prx4 (4, 8 and 16 μg). After 0.5 and 2 h incubation at room temperature, nicking of the supercoiled plasmids by hydroxyl radical from metal-catalyzed oxidation (MCO) assay was evaluated on 0.8% agarose gel electrophoresis.

Cumulative mortality assay on *LvPrx4* silenced- or r*Lv*Prx4 injected-shrimp

To understand the function of *Lv*Prx4 on VP_{AHPND} resistance in shrimp, *LvPrx4* silencing was performed using RNAi technique. The dsRNAs specific to *LvPrx4* (dsPrx4) and GFP (dsGFP) as a control were prepared. Gene-specific fragment coding for dsRNA was amplified by specific primers (Table S1) and cloned into pET19b vector. The recombinant plasmid was transformed into *E. coli* HT115. The dsRNA was produced and purified according to the previous report.[60] Shrimp were injected with 20 μg/g shrimp dsPrx4, 20 μg/g shrimp dsGFP or 0.85% NaCl. After 24-h post-injection, hemocytes of three individuals each were collected to check the efficiency of knockdown by qRT-PCR. Then, the VP_{AHPND} culture was added to tanks containing ten shrimps and the shrimp cumulative mortality was observed.

To study the effect of the r*Lv*Prx4 protein on shrimp tolerance to VP_{AHPND} infection. Shrimp were injected with 2 nmol/g shrimp r*Lv*Prx4, 2 nmol/g shrimp rGST or 20 mM Tris pH 8.0 buffer. After 24-h post-injection, shrimp were challenged with VP_{AHPND} as described above.

Bacterial counting and binary Pir toxin copy number quantification

To study the total bacteria in hemolymph and hepatopancreas after VP_{AHPND} infection in r*Lv*Prx4-pretreated shrimp. Shrimp were injected with 2 nmol/g shrimp r*Lv*Prx4, 2 nmol/g shrimp rGST or 20 mM Tris pH 8.0. After 24 h post-injection, shrimp were challenged with 5×10^5 CFU/mL VP_{AHPND} by immersion. After 0, 24 and 48 h post-VP_{AHPND} challenge, shrimp hemolymph and hepatopancreas were individually collected from three shrimps and the number of bacteria was determined by dotting on TCBS selective agar plate. The total number of colonies (CFUs) were counted after incubation at 30°C overnight.

To quantify the copy number of binary Pir toxin, hemocytes and hepatopancreas after VP_{AHPND} injection were extracted the gDNA. The copy number of binary Pir toxin was determined using extracted gDNA as template by qRT-PCR with specific primer to TUMSAT-VP3 (Table S1) which includes the part of binary Pir toxin sequence.

Determination of H_2O_2 level in the VP_{AHPND}-challenged shrimp

Hemocytes and hepatopancreas of VP_{AHPND}-challenged shrimp as described above were individually collected from three shrimps, homogenized in 50 mM potassium phosphate buffer pH 7.0 and centrifuged at 6,000xg for 15 min. Supernatant was mixed with 1% (V/V) $TiCl_4$ in conc. HCl and incubated in darkness for 15 min followed by centrifugation at 6,000xg for 15 min. Absorbance at 410 nm was monitored.

Effect of the r*Lv*Prx4-injected shrimp on the expression of the immune-related genes in hemocyte and on PO activity in hemolymph

Shrimp were injected with 1 nmol/g shrimp r*Lv*Prx4, 2 nmol/g shrimp r*Lv*Prx4, 2 nmol/g shrimp rGST or 20 mM Tris-Cl pH 8.0 and then shrimp hemocytes were collected after 24 h post-injection. Hemocytes were subjected to the total RNA extraction and cDNA synthesis. The expression level of the immune-related genes was determined by qRT-PCR with specific primers (Table S1).

Hemolymph of r*Lv*Prx4-injected shrimp as described above was measured PO activity. Briefly, the hemolymph was mixed with 25 mM Tris-Cl pH 8.0 and 3 mg/mL L-DOPA in water (Sigma). The absorbance at 490 nm was monitored for 2 h. The PO activity was calculated as ΔA_{490}/mg protein/min.

Co-localization of r*Lv*Prx4 and *Lv*TLR

HEK293T cells were cultured in DMEM and seeded into a 24-well plate, then co-transfected with 400 ng of r*Lv*Prx4 expression plasmid, pRL-CMV, and 400 ng of plasmid expressing leucine rich repeat (LRR) domain of *Lv*TLR1, pEGFP-N1, or *Lv*TLR2, pEGFP-N1, fused with green fluorescence protein EGFP (*Lv*TLR1_LRR-EGPF or *Lv*TLR2_LRR_EGFP) using Lipofectamine 3000 in Opti-MEM for 48 h. Cells were fixed and stained with Cell Brite cytoplasmic membrane dye and rabbit polyclonal anti-*Lv*Prx4 antibody followed by addition of anti-rabbit secondary antibody conjugated with Alexa Fluor 568. *Lv*TLR1 and 2 were detected as green fluorescence. The nuclei were stained with Hoechst 33342 and fluorescence images were detected with LSM 900 laser scanning confocal microscope (Carl Zeiss).

Localization of r*Lv*Prx4 on TLR-silencing hemocytes by immunofluorescence

To identify the r*Lv*Prx4-interacting protein that aids innate immune induction in shrimp, *Lv*TLR1 and *Lv*TLR2 expressed in hemocyte were suppressed using RNAi interference and the r*Lv*Prx4 introduced into shrimp was detected by immunofluorescence. Gene-specific fragment coding for dsRNA was cloned into vector L4440. The dsRNA was expressed in *E. coli* HT115. Shrimp were injected with dsTLR1 (20 μg/g shrimp), dsTLR2 (20 μg/g shrimp), dsGFP (20 μg/g shrimp) or 0.85% NaCl. After 48-h post-injection, hemocytes were collected to check the efficiency of knockdown by qRT-PCR and then shrimp were injected with r*Lv*Prx4 at 2 nmol/g shrimp or 20 mM Tris-Cl pH 8.0 buffer. Hemocytes were fixed and stained with Cell Brite cytoplasmic membrane dye and mouse monoclonal anti-His antibody followed by addition of anti-mouse secondary antibody conjugated with Alexa Fluor 488. The nuclei were stained with Hoechst 33342. Fluorescence images were detected with LSM 900 laser scanning confocal microscope (Carl Zeiss).

In vitro pull-down of *Lv*Prx4 with *Lv*TLR1 and 2

HEK293T cells were transfected with plasmid expressing *Lv*TLR1_EGFP, *Lv*TLR1_LRR-EGFP, *Lv*TLR2_EGFP, *Lv*TLR2_LRR_EGFP or Renilla *Luciferase* (RL)_EGFP (control protein) and then lysed with lysis buffer (20 mM Tris pH 8.0, 150 mM NaCl, 1% (w/v) Triton X-100 and 1 mM PMSF). Cell lysates were incubated with Ni-NTA beads pre-incubated with r*Lv*Prx4. After washing the beads, interacting proteins were eluted with elution buffer (20 mM Tris-Cl pH 8.0 and 500 mM imidazole) and analyzed using SDS-PAGE and Western blotting.

Identification of r*Lv*Prx4-induced pathway using RNAi interference

This experiment aims to verify if Toll pathway is the immune pathways that are triggered by r*Lv*Prx4 challenge. The *Lv*TLR1 and *Lv*TLR2 were suppressed using RNAi interference as described above. After 48-h post-r*Lv*Prx4 challenge, shrimp were injected with 2 nmol/g shrimp or 20 mM Tris-Cl pH 8.0 buffer for the control group. The same set of selected genes were analyzed for their expression levels in hemocytes of shrimp after 24 h-post r*Lv*Prx4 challenge using qRT-PCR.

QUANTIFICATION AND STATISTICAL ANALYSIS

The experiments of cell death assay *in vitro* and *in vivo*, qRT-PCR, protein quantification, peroxidase activity, PO activity, cumulative mortality assay and bacterial counting were performed in triplicate. The results were expressed as the mean ± SD. Data were analyzed using one-way ANOVA followed by Duncan's new multiple ranges test for qRT-PCR, PO activity and bacterial counting while a paired-samples t-test was used for cell death assay, protein quantification and peroxidase activity. The statistical significance was accepted at the $p < 0.05$. Cumulative mortality assay was analyzed by GraphPad Prism 9 using Log rank (Mantel-Cox) test and are presented as mean ± SE at each time point.